



# Dynamic Electrochemical Promotion of Catalysis

Shrinjay Sharma

Delft University of Technology



# Dynamic Electrochemical Promotion of Catalysis

by

**Shrinjay Sharma**

in partial fulfillment of the requirements for the degree of

**Master of Science**  
in Mechanical Engineering

at the Delft University of Technology,  
to be defended on Thursday August 27, 2020 at 9:00 AM.

Student number:	4899245
Project duration:	Novembet, 2019 – August, 2020
Thesis Committee:	Prof. dr. ir. Earl Goetheer, TU Delft, Supervisor
	Prof. dr. ir. Thijs Vlugt, TU Delft
	Dr. Ruud Kortlever, TU Delft
	Ir. Jasper A Ros, TNO



# Acknowledgement

My heartfelt gratitude goes towards my supervisor, Prof.dr.ir. Earl Goetheer for giving me the opportunity to work under him. It was a great learning experience for me. I am grateful to him for his constant support and guidance without which it would have not been possible for me to complete my thesis. I also thank him for all the frequent discussions we had on the thesis. That helped me a lot to stay on track.

I am grateful to Prof.dr.ir. Thijs Vlugt and Dr. Ruud Kortlever for their consent to be the members of my graduation committee.

I am also thankful to Jasper. A. Ros from *TNO* for the fruitful discussions and the valuable suggestions on my report. Next, I would like to thank Dr. ir. Leon. F. Geers from *TNO* for his help in my modelling work. It helped me a lot in getting the desired results.

Lastly, I am grateful to my family for their both emotional and financial support throughout these two years. Their love and encouragement has helped me keep moving even in my difficult times.

*Shrinjay Sharma*  
*Delft, August 2020*



# Abstract

Electrochemical Promotion of Catalysis (*EPOC*) is a method for enhancing a catalytic reaction by modifying the surface properties of the catalyst through the application of a small amount of current or interfacial potential. It can also be used to enhance the selectivity of heterogenous catalytic reactions. It was first discovered by *M. Stoukides* and *C. Vayenas* in early 1980s. This phenomenon can increase the catalytic rate by 10 to  $10^5$  times compared to the electrochemical rate of supply of ions to the catalyst which is given by Faraday's law. Therefore, the process is no longer faradaic and hence, it is also known as "Non-Faradaic Electrochemical Modification of Catalytic Activity (*NEMCA*)".

Today, the *EPOC* mechanism has been widely researched by different research groups, and many reactions have been investigated, but unfortunately, no commercial application of the technology is available. The main problem with *EPOC* is the lower activity per unit mass of the catalyst compared to the commercially used catalysts in conventional reactors. This drawback has been hindering the commercialisation of this idea.

A new route has been proposed, which is called "Dynamic Electrochemical Promotion of Catalysis (*DEPOC*)". The difference between *EPOC* and *DEPOC* comes from the dynamic operation of the system. In *DEPOC*, the current or the potential over the catalyst is varied periodically at different frequencies, symmetries and amplitudes of the wave-forms. This periodic modification is expected to have a role on selectivity of products and reaction rate.

The main application that is considered for this mechanism is the Fischer-Tropsch (*FT*) reaction. It is a polymerization process which leads to hydrogenation of carbon monoxide forming liquid hydrocarbons. Controlling the selectivity of this reaction is hard, and normally a wide distribution of carbon chain lengths are obtained. With periodic application of voltage on the *DEPOC* catalyst, it is expected to be able to control the selectivity of the reaction it is expected to be able to control the selectivity of the reaction or in other words the product distribution of the reaction.

In this thesis, the *DEPOC* effect will be mainly studied from a theoretical perspective. First, the *EPOC* phenomenon will be analysed and the theory will be extended to the *DEPOC* effect. The study will be based on understanding the thermodynamics and the kinetics of these mechanisms. Lastly, a conceptual reactor design approach will be studied for the process.

*Shrinjay Sharma*  
*Delft, August 2020*



# Contents

<b>List of Figures</b>	<b>ix</b>
<b>List of Tables</b>	<b>xi</b>
<b>1 Introduction</b>	<b>1</b>
1.1 Background . . . . .	1
1.2 Catalysis . . . . .	2
1.3 Electrochemical Promotion of Catalysis . . . . .	3
1.4 Periodic Operation . . . . .	4
1.5 Research Questions . . . . .	6
1.6 Modelling Approach . . . . .	6
1.7 Thesis Outline . . . . .	7
<b>2 Literature Review</b>	<b>9</b>
2.1 Electrochemical Promotion of Catalysis . . . . .	9
2.1.1 Thermodynamics . . . . .	10
2.1.2 Promotional Rules . . . . .	11
2.1.3 Reaction Kinetics . . . . .	13
2.1.4 Commonly Used Terms . . . . .	14
2.1.5 Promoter Ions . . . . .	15
2.1.6 <i>EPOC</i> , Classical Promotion and Metal Support Interaction . . . . .	15
2.1.7 Effect of <i>EPOC</i> on different reactions . . . . .	16
2.1.8 <i>EPOC</i> in Hydrogenation Reaction . . . . .	16
2.2 Fischer Tropsch Reaction . . . . .	17
2.2.1 Reaction Kinetics . . . . .	17
2.2.2 Product Distribution . . . . .	19
2.2.3 Effect of Temperature . . . . .	19
2.2.4 Effect of Alkali Promotion . . . . .	20
2.2.5 Periodic Operation in Fischer Tropsch . . . . .	20
<b>3 Modelling</b>	<b>23</b>
3.1 Surface Coverage of Promoter Ions . . . . .	23
3.2 <i>EPOC</i> in Fischer Tropsch . . . . .	24
3.2.1 Charge Transfer Coefficient . . . . .	24
3.2.2 Chain Growth Probability . . . . .	25
3.2.3 Reaction Rate . . . . .	26
3.2.4 Olefin-Paraffin Ratio . . . . .	27
3.2.5 Continuous Stirred Plug Flow Reactor . . . . .	28
3.3 Application of Periodic Potential . . . . .	29
3.3.1 Transport of Ions . . . . .	29
3.3.2 Periodic Electrochemical Promotion of Catalysis for Fischer Tropsch Reaction . . . . .	29
3.4 Solid Oxide Fuel Cell ( <i>SOFC</i> ) type Reactor . . . . .	30

<b>4</b>	<b>Results and Discussions</b>	<b>35</b>
4.1	Surface Coverage of Promoter Ion	35
4.2	Electrochemical Promotion of Catalysis on Fischer Tropsch Reaction.	36
4.2.1	Chain Growth Probability	36
4.2.2	Reaction Rate	36
4.2.3	Olefin-Paraffin Ratio	37
4.3	Combined Effect of Operating Conditions and <i>EPOC</i> on <i>FT</i>	38
4.3.1	Temperature + <i>EPOC</i>	39
4.3.2	$H_2 : CO$ Ratio + <i>EPOC</i>	39
4.3.3	Pressure + <i>EPOC</i> .	40
4.4	Dynamic Electrochemical Promotion of Catalysis	41
4.4.1	Effect of Frequency.	41
4.4.2	Effect of Duty Cycle	44
4.4.3	Effect of Amplitude	45
4.5	Reactor Design Philosophy.	47
4.5.1	Catalyst for <i>EPOC</i>	47
4.5.2	Wireless Configuration.	47
4.5.3	Reactant Conversion for Fischer Tropsch reaction	47
4.5.4	Importance of Heat Management in Fischer Tropsch	48
<b>5</b>	<b>Conclusion and Future Outlook</b>	<b>51</b>
5.1	<i>EPOC</i> in Fischer Tropsch.	51
5.2	Dynamic Electrochemical Promotion of Catalysis	52
5.3	Reactor Design	52
5.4	Future Outlook.	53
	<b>Bibliography</b>	<b>55</b>

# List of Figures

1.1	Increase in atmospheric CO <sub>2</sub> content in the atmosphere. . . . .	1
1.2	Research on CO <sub>2</sub> reduction at different scales. . . . .	2
1.3	Sabatier's Volcano Plot. . . . .	3
1.4	Sodium ion as promoter in an EPOC cell for a hypothetical reaction $A + B \rightarrow P$ . . . . .	3
1.5	Square Wave forms with different Duty Cycles. . . . .	4
1.6	Variation of Average turn over frequency with frequency of oscillations of binding energy for hypothetical reaction ( $A \rightarrow B$ ). . . . .	5
1.7	Variation of weight fractions of different lengths of carbon chains as a function of chain growth probability. . . . .	6
2.1	Anionic and Cationic transport of ions to the catalyst surface. . . . .	9
2.2	Back-spillover of Na <sup>+</sup> ions on the catalyst surface. . . . .	10
2.3	Electrophobic . . . . .	11
2.4	Electrophilic . . . . .	12
2.5	Volcano . . . . .	12
2.6	Inverted Volcano . . . . .	13
2.7	Variation of reaction rate with H <sub>2</sub> : CO ratio. . . . .	19
2.8	Weight fraction of FT products at different temperatures. . . . .	20
3.1	Side and Top View of SOFC type unit reactor cell for EPOC . . . . .	31
4.1	Change in surface coverage of promoter ion (Na <sup>+</sup> ) with the catalyst potential. . . . .	35
4.2	Variation of chain growth probability with different catalyst potentials using equations by Song <i>et al</i> and Vervloet <i>et al</i> . . . . .	36
4.3	Effect of changing catalyst potential on the overall reaction rate. . . . .	37
4.4	Variation of olefin – paraffin ratio for C <sub>2</sub> wrt catalyst potential. . . . .	37
4.5	Carbide Mechanism for FT reaction. . . . .	38
4.6	Variation of olefin – paraffin ratio for C <sub>2</sub> , C <sub>3</sub> and C <sub>5</sub> wrt catalyst potential. . . . .	38
4.7	Variation of chain growth probability and reaction rate with different temperatures and catalyst potentials. . . . .	39
4.8	Variation in Selectivity of C <sub>1</sub> , C <sub>2</sub> and C <sub>3</sub> as a function of temperature at an applied catalyst potential of –0.4V. . . . .	39
4.9	Variation of reaction rate and chain growth probability with H <sub>2</sub> : CO ratio at different catalyst potentials. . . . .	40
4.10	Variation of reaction rate and residence time as a function of pressure. . . . .	40
4.11	Effect of pressure on chain growth probability at different catalyst potential. . . . .	41
4.12	Variation of promoter coverage on the surface of a catalyst film of thickness 0.1 μm at frequencies of 0.01 Hz and 0.01 Hz. . . . .	42
4.13	Variation of promoter coverage on the surface of a catalyst film of thickness 1 μm at frequencies of 0.01 Hz and 0.01 Hz. . . . .	42
4.14	Input signal of catalyst potential . . . . .	42
4.15	Effect of frequency on CO conversion . . . . .	43
4.16	Variation of CH <sub>4</sub> selectivity and C <sub>2</sub> H <sub>4</sub> : C <sub>2</sub> H <sub>6</sub> ratio with increasing frequency of oscillations of the catalyst potential waveform. . . . .	43
4.17	Variation of CO conversion and C <sub>2</sub> H <sub>4</sub> : C <sub>2</sub> H <sub>6</sub> ratio with increasing duty cycle. . . . .	44

---

4.18	Variation of chain growth probability and selectivity of $CH_4$ as a function of duty cycle. . . . .	45
4.19	Variation of $CO$ conversion and $C_2H_4 : C_2H_6$ ratio as functions of the amplitude of the input potential square wave. . . . .	46
4.20	Variation of chain growth probability and selectivity of $CH_4$ as functions of the amplitude of the input potential square wave. . . . .	46
4.21	Consumption of reactants along the length of the reactor using modified reaction rate to account for the low catalytic activity in the case of <i>EPOC</i> and the original <i>Yates</i> and <i>Satterfield</i> expression. . . . .	48
4.22	Consumption of reactants along the length of the reactor using catalyst common to <i>EPOC</i> and that used in conventional <i>FT</i> reactors. . . . .	48

# List of Tables

2.1	Promoter ions and their corresponding electrolyte materials . . . . .	15
2.2	Reactions performed using <i>YSZ</i> electrolyte and $O^{2-}$ promoter ion . . . . .	16
2.3	Reactions performed using $\beta'' Al_2O_3$ electrolyte and $Na^+$ promoter ion . . . . .	16
2.4	Parameters used in <i>Post et al</i> expression:2.16 . . . . .	18
2.5	Parameters used in <i>Yates and Satterfield</i> expression:2.17 . . . . .	18
2.6	Parameters used in expression:2.18 . . . . .	18
3.1	Constants for equation:3.6 . . . . .	26
3.2	Constants for equation:3.7 . . . . .	26
3.3	Constants for equation:3.9 . . . . .	27
3.4	Values of the parameters $k_i$ , $m$ and $n$ used in equation: 3.16c . . . . .	30
3.5	Thermal conductivities for different components of the reactor:3.20 . . . . .	32
3.6	Constants for equation:3.20 . . . . .	32
4.1	Constants for equation:3.9 . . . . .	41
4.2	Comparison between <i>DEPOC</i> and <i>EPOC</i> . . . . .	45
4.3	Maximum and minimum catalyst potentials corresponding to different amplitudes for a symmetrical square wave. . . . .	45



# Nomenclature

## Physical Constants

$\epsilon_0$	Permittivity of free space	$8.85 \cdot 10^{-12} [CV^{-1}m^{-1}]$
$e$	Charge of an electron	$1.6 \cdot 10^{-19} [C]$
$F$	Charge of one mole of electron	$96485 [C/mol]$
$k_b$	Boltzmann's Constant	$1.38 \cdot 10^{-23} [J/K]$
$R$	Universal Gas Constant	$8.314 [J/(mol K)]$

## Acronyms

*ASF* Anderson Schulz Flory

*CSTR* Continuous Stirred Tank Reactor

*DEPOC* Dynamic Electrochemical Promotion of Catalysis

*EPOC* Electrochemical Promotion of Catalysis

*FT* Fischer Tropsch

*LHHW* Langmuir Hinshelwood Hougen Watson

*MSI* Metal Support Interaction

*NEMCA* Non-Faradaic Electrochemical Modification of Catalytic Activity

*SOFC* Solid Oxide Fuel Cell

*YSZ* Yttria stabilized zirconia



# Chapter 1

## Introduction

### 1.1 Background

$CO_2$  level in the atmosphere is rising at an alarming rate, which is one of the prime cause for global warming. Consequently, it has led to increase in temperature, melting of ice, rising sea levels and has become a threat to the entire ecosystem. As per the latest reports from *Mauna Loa Observatory*, at present,  $CO_2$  level has increased to around 420 ppm<sup>1</sup>. The trend has been ever increasing which can be seen from fig: 1.1. Because of the rising concerns with  $CO_2$  emissions from industries, its capture, storage and utilisation has been studied for several decades by different research groups. With the passage of time, it has also started to attract the attention of the industries.

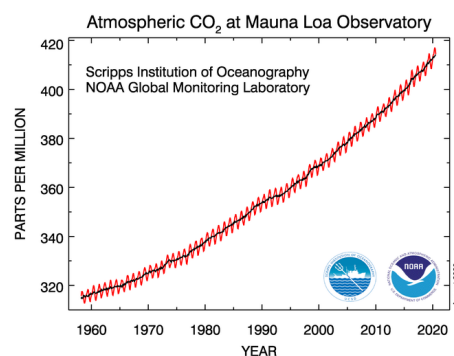


Figure 1.1: Increase in atmospheric CO<sub>2</sub> content in the atmosphere.

$CO_2$  capture is mainly done through post combustion capture, oxy-fuel combustion capture and pre-combustion capture. Post combustion capture can be done through separation processes.  $CO_2$  is separated from flue gases or other sources by adsorption, absorption, membrane separation processes, or using gas hydrate technologies [1]. In oxy-fuel combustion, oxygen is used instead of air for the purpose of combustion [2]. The flue gas contains mainly  $CO_2$  and  $H_2O$ . The latter can be separated through condensation. In pre-combustion capture, fuel is partially oxidised to  $CO$  and  $H_2$  and then the produced  $CO$  is oxidised with steam to form  $CO_2$  [3]. Direct Air Capture is another way of capturing  $CO_2$ . It is done by separating  $CO_2$  from ambient air rather than capturing from sources like industry effluents, biomass power plants, or cement factories [4]. Storage of captured  $CO_2$  in large geological formations is called sequestration [5]. It is stored in the form of mineral carbonates.

Another attractive option is to convert the captured  $CO_2$  to methanol [6] or other synthetic fuels via hydrogenation. One of the ways to produce these hydrocarbons is through electrolysis. Aqueous phase electrolysis performed at room temperature can produce a range of different hydrocarbons depending on the conditions and the type of catalysts used [7].  $CO_2$  can also be used in high temperature electrolysis in a solid oxide cell [8]. But in solid oxide electrolysis  $CO$  is the only product. Therefore, a second step will be required to convert

<sup>1</sup><https://www.esrl.noaa.gov/gmd/ccgg/trends/>

it into synthetic fuels. Fischer Tropsch reaction could be a possible down-stream process in this regard [9]. Electrochemical reduction of  $CO_2$  is an interdisciplinary topic which has been researched to a great extent. Still more to be done in this field. The research on  $CO_2$  reduction encompasses a broad spectrum of scales from molecular level ( $nm$  scale) to the plant level ( $km$  scale). Figure: 1.2 shows different scales at which research on  $CO_2$  reduction is done <sup>2</sup>. It also includes the number of papers published at each scale.

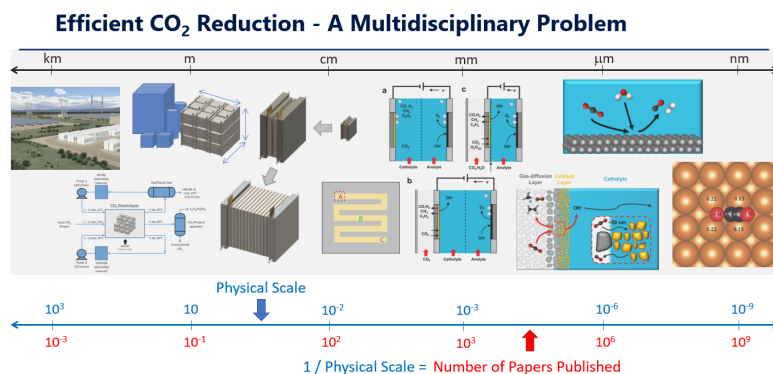


Figure 1.2: Research on  $CO_2$  reduction at different scales.

Alternate methods for producing synthetic fuels or hydrocarbons has become necessary as fossil-based resources or oil reserves are depleting [10]. This gives another reason to focus on Fischer-Tropsch (*FT*) which can produce hydrocarbons through polymerisation process. It is a  $CO$  hydrogenation process. Traditionally  $CO$  is obtained from natural gas, biomass or coal gasification [10]. As stated above,  $CO$  can be produced through  $CO_2$  electrolysis. Co-electrolysis is another option in which both  $CO$  and  $H_2$  can be produced simultaneously which can be used in downstream processes like the *FT* [11]. Apart from the ability to simultaneously produce  $CO$  and  $H_2$ , co-electrolysis operates at a lower input potential than  $CO_2$  electrolysis.

Fischer Tropsch reaction is known to have a broad product distribution. Therefore, selectivity is one of the major issues with this reaction. Operating conditions like temperature and feed ratio, do affect the selectivity [12]. Apart from which, the role of catalysts and promoters is also very crucial on selectivity [13].

## 1.2 Catalysis

Catalysts are substances which are used in the reactions either to accelerate the process, modify the outcome of the reaction or both without themselves getting consumed. Catalysis can be both homogeneous and heterogeneous. Homogeneous catalysts are those which are in the same phase as the reactants and products, whereas heterogeneous catalysts are those which are in a phase different from the reactants and the products. Heterogeneous catalysts are more commonly used. Out of innumerable reactions, few industrial examples are Iron-Chromium or Copper-Zinc as a catalyst for water gas shift reaction [14], Iron oxides on Alumina for Haber Bosch Process [15], Nickel for steam reforming of Methane [16], etc.

Electrocatalysts are those which participate in an electrochemical reaction by assisting the transfer of electrons between the electrode and the reactants. These catalysts can also be categorised as homogeneous (e.g., coordination complex or enzyme) [17] and heterogeneous (e.g., platinum, copper) [18], [7].

According to the Sabatier principle, "In order to have high catalytic activity, the interaction between reactants and catalysts should neither be too strong nor too weak. If the interaction is too weak, then there will be no reaction on the surface as it will be difficult for catalytic surfaces to bind the reactants. If the interaction is too strong, then the products will not readily desorb from the catalytic surface, lowering the activity of the surface" [19]. This principle can be described by volcanic plots between the bond strength and reaction rate.

<sup>2</sup>By courtesy of Tom Burdyny, Assistant Professor, Materials for Energy Conversion and Storage group, Department of Chemical Engineering, TU Delft

Catalysts which lie in the vicinity of the volcano peak are optimum for the given reaction [20]. Figure: 1.3 shows a typical volcanic plot between the reaction rate and surface binding energies.

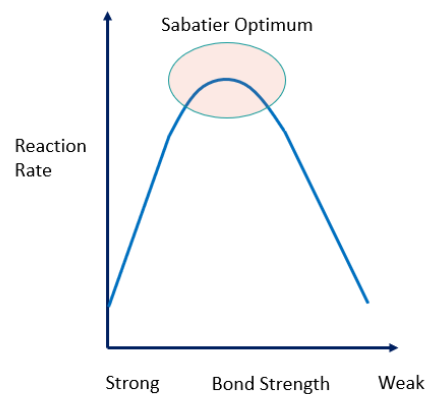


Figure 1.3: Sabatier's Volcano Plot.

Often promoters are added to the catalyst for further improvement in activity or selectivity of the reaction. Promoters modify the intrinsic kinetics of the reaction and also the adsorption strength of the reactants [21]. Promoters can be added via classical promotion or metal support interaction. Another novel way of adding promoter ions to the catalyst surface is through electrochemical promotion of catalysis. Similarities and differences among the three techniques will be discussed in subsection: 2.1.6 in Chapter: 2.

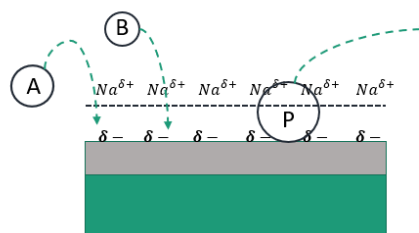


Figure 1.4: Sodium ion as promoter in an EPOC cell for a hypothetical reaction  $A + B \rightarrow P$ .

### 1.3 Electrochemical Promotion of Catalysis

Electrochemical Promotion of Catalysis (EPOC) is a method for enhancing a catalytic reaction by modifying the surface properties of the catalyst through the application of a small amount of current or interfacial potential [21]. It is mainly performed in a solid oxide fuel cell type reactor cell. When there is a potential difference between the catalyst and the counter electrode, then the electrochemically generated ions are transported to the catalyst surface and back-spillover of these ions take place on the surface [22]. Both anions and cations can be used as promoters.

This phenomenon was first discovered by *M. Stoukides* and *C. Vayenas* in the early 1980s [21]. It can increase the catalytic rate by  $10^1$  to  $10^5$  times compared to the electrochemically generated ions which obey *Faraday's law* [21]. Therefore, the process is no longer faradaic. Thus, it is also known as "Non Faradaic Modification of Catalytic Activity". This effect has been tested on a wide variety of reactions [22].

A double layer is formed by the adsorbed promoters which modify the work function of the catalyst surface [22]. Figure: 1.4 shows the double layer formed by the *Na* atoms adsorbed on the catalyst surface. Further, interaction of the reactants of a given reaction with this catalyst surface changes their respective adsorption

strength. Consequently, the change in the adsorption strengths will influence the reaction rate [23]. Apart from adsorption, the transition state of the surface reactions and the desorption of the products can also experience the effect of this double layer [23].

Solid state reactors are commonly used for studying this effect. Commonly studied reactions are *CO* oxidation [24], *Ethylene* oxidation [25], *NO* reduction [26]. Apart from solid state reactors, aqueous phase or liquid electrolyte based reactors are also investigated. *H<sub>2</sub>* oxidation [27], [28] and *CO<sub>2</sub>* reduction on *Palladium* based gas diffusion electrodes [29] are two of the few examples. *NEMCA* in aqueous phase reactors do not require back spill over of ions on the catalyst surface [21]. The transport of ions take place in a similar way to that of aqueous phase electrochemical reactions. The research is not extensively done as in solid state devices and also there is lack of theoretical studies done on the effect of *EPOC* in reactions performed in aqueous phase or liquid electrolyte based reactors.

The study of *EPOC* has been done in steady and transient state [30]. But no study has been found in the literature on the periodic application of the *EPOC* effect evaluating the frequency, amplitudes and the symmetry of the input potential waveforms. One of the major motivations for periodic operation lies in its kinetics [31]. Improving the selectivity is one of the main goals for which periodic operations are performed. Moreover, the demand for renewable energy is increasing but it has an intermittent nature. Therefore, dynamic operation of processes can play a major role in the future and studying periodic operation can be a step in understanding the effects of dynamic operation on different processes.

## 1.4 Periodic Operation

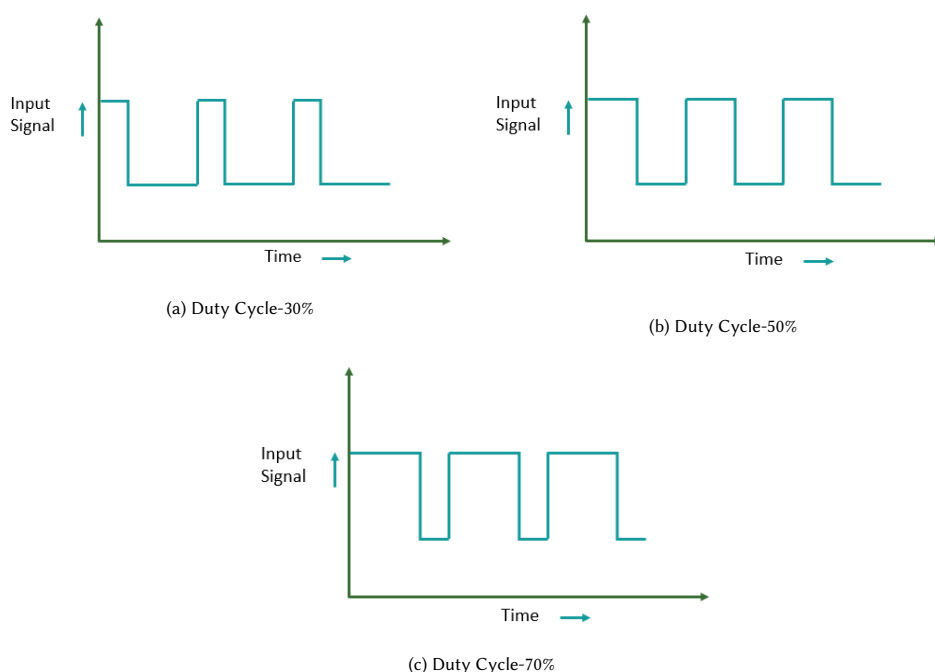


Figure 1.5: Square Wave forms with different Duty Cycles.

Periodic operation is done to enhance the performance of the catalytic reactor in terms of reactant conversion, selectivity of product, catalyst activity maintenance, longer catalyst life, higher product recovery, prevention of thermal runaway, etc. Improvement on such grounds due to periodic operation can contribute in reducing capital and operating costs [32]. Different input parameters can be varied periodically. Flow reversal, variation in feed composition, temperature and pressure variations, etc are some ways to introduce periodicity to a process [32].

Pulsating flow techniques can be used to overcome mass transport limitations in chemical processes. Low mass transfer of the reactants towards the catalytically active surface is one of the major drawbacks of the electrochemical processes. *Gallent et al* studied the effect of pulsating flow on the oxidation of 1,2-propanediol to lactic acid and pyruvic acid [33]. On application of pulsation to the flow, they reported increased production of lactic acid. Periodic operations are also used for industrial applications like pressure swing adsorber for separation process, pulsed electroplating, etc. Pulsed electroplating or deposition is a process where the thickness and the composition of the deposited metal coatings or films are controlled by the alternate application of current [34].

Various waveforms like square, sinusoidal, saw tooth and triangular type are used to create pulsation of input parameters. Effect of pulsation depends on its waveform, amplitude, frequency of the periodicity and duty fraction. Duty fraction or symmetry of a cycle is defined as the ratio between the pulse duration and the time period of the wave form. Fig: 1.5 shows square wave forms with different duty cycles. Optimal choice of these parameters can have a positive effect on the process over its steady state counterpart. For a periodic operation, the choice of the time period is important. It depends on the important time scales of the concerned process. For example, in a reaction, the time scale for reactant adsorption, surface reaction, product desorption and diffusion of reactants and products inside the reactor have to be considered.

Application of pulsed potential or current on electrolysis has been researched for improvement in selectivity of products or enhancement in reaction rate. Common reactions found in literature are electroreduction of nitrobenzene, phenol oxidation and water electrolysis. *Fedkiw* and *Scott* have reviewed the role of pulse electrolysis on the selectivity of electro-organic reactions [35]. *Fedkiw* and *Chao* reported the selectivity of the electroreduction of nitrobenzene [36]. Electroreduction of Nitrobenzene forms an intermediate Phenylhydroxylamine (*PHA*) which can further form Aniline, electrochemically and p-Aminophenol chemically [36]. The authors have shown that the use of suitable waveform and controlling the frequency of the pulses could have an impact on the selectivity of the *PHA*. *Reitlinger* has shown the selectivity of oxidation of ethyl alcohol towards acetaldehyde [37]. Further oxidation towards acetic acid was suppressed due to the application of alternating current. In these electro organic reactions, selectivity could be modified because the intermediates and the products have different kind of interactions with the applied potential.

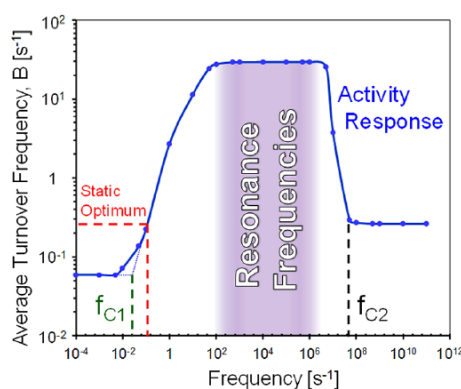


Figure 1.6: Variation of Average turn over frequency with frequency of oscillations of binding energy for hypothetical reaction ( $A \rightarrow B$ ).

Periodicity in operating conditions like feed ratio ( $H_2 : CO$  ratio) and temperature were also studied on *FT* reaction. A discussion on this topic has been done in section: 2.2.5 in Chapter: 2. Another important discovery related to periodic study is the catalytic resonance. *Ardagh et al* showed that if the binding energy of the catalyst is oscillated between two energy states, its productivity can go beyond the Sabatier optimum [38]. The maximum productivity or the turnover frequency is reached when the frequency of the oscillations resonates with the natural frequency of the chemical kinetics. This phenomenon is called catalytic resonance. Figure: 1.6 shows the resonance phenomenon for a hypothetical reaction ( $A \rightarrow B$ ) produced by *Ardagh et al* [38]. Using catalytic resonance theory, *Ardagh et al* also showed that selectivity of parallel reactions ( $A \rightarrow B$  &  $A \rightarrow C$ ) can be tuned towards one of the products which is not possible at steady state operation [39].

## 1.5 Research Questions

*FT* reaction is known to produce a wide distribution of products. Narrowing down the product range is one of the major challenges of the reaction. Methane and heavy wax can have 100% selectivity with extreme cases of low and high probability for the growth of the carbon chains as shown in figure: 1.7 [40]. But middle distillates are always accompanied by methane and wax formations. Therefore, this challenge makes it interesting to look for ways to improve the selectivity of the reaction. Influence of *EPOC* on selectivity of reactions has already been studied. There are experimental studies on understanding the effect of promoter ions on the selectivity of  $NO_x$  reduction using  $CO$  or  $C_3H_6$  [26],  $CO_2$  hydrogenation [41], etc. Also, the effect of electrochemical promotion on *FT* reaction has been studied experimentally to understand its role on reaction rate and product selectivity. But so far no theoretical study on the effect of *EPOC* on *FT* has been done. Also, the influence of periodic application of the promotion effect on *FT* reaction has not been studied yet.

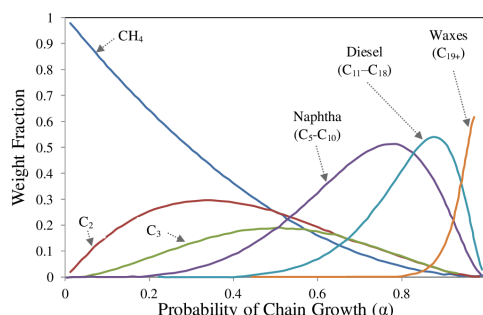


Figure 1.7: Variation of weight fractions of different lengths of carbon chains as a function of chain growth probability.

Based on these ideas, the following questions have been addressed in this thesis.

- What modifications are necessary on the existing equations to study *FT* reaction in order to capture the influence of the electrochemically generated promoters on the process?
- What difference can be observed in the selectivity and productivity of the *FT* reaction due to the periodic application of the promotional effect over steady state application?
- What are the important factors to be considered while designing a reactor for electrochemically promoted *FT* reaction?

To find the answers of the above questions, the study has been carried out in three phases:

- Understanding the effect of *EPOC* on *FT* via theoretical modelling and compare the results with those obtained through experiments in literature. The aim is to implement the existing equations used in the study of the *FT* process with necessary modifications to capture the *EPOC* effect.
- Study the impact of periodic application of electric potential on the *FT* reaction.
- Exploring the reactor design concepts for scaling up of such systems.

## 1.6 Modelling Approach

The study has been carried out theoretically using various modelling approaches. Firstly, the effect of *EPOC* on *FT* has been studied using analytical or semi empirical equations. Modifications to these existing equations have been made so that they can account the effect of the applied potential on the reaction. Further, plug flow continuously stirred tank reactor (*CSTR*) model has been created to understand the effect of periodic application of potential. Lastly, one dimensional steady state plug flow reactor has been used to study the performance of the process inside an *SOFC* type reactor.

## 1.7 Thesis Outline

This section gives a short glimpse about the content present in each chapter.

Ch:2 briefly outlines the research carried out in the past on Electrochemical Promotion of Catalysis and Fischer Tropsch reaction.

Ch:3 describes the modelling approaches adopted to study the phenomenon. It includes zero dimensional models which are mostly based on semi-empirical or analytical expressions. Also, one dimensional models were created based on ordinary differential equations to study the periodic operation and reactor concepts.

Ch:4 includes the results and discussions obtained based on the modelling approaches discussed on 3.

Ch:5 concludes the important findings through this study and talks about the prospects this topic carries for future research.



# Chapter 2

## Literature Review

### 2.1 Electrochemical Promotion of Catalysis

As defined in Chapter:1, electrochemical promotion of catalysis (*EPOC*) modifies the catalyst surface through the back spillover of electrochemically generated ions which brings a change to the reaction taking place on the surface. After the discovery of *EPOC*, a significant number of reactions have been studied till date [21]. Improvement in reaction rate compared to the case without the application of potential or current was reported almost in most of the cases [22]. In other words, improvement in the reaction rate could be seen due to the presence of electrochemically generated promoters. Reactions with more than one product also experienced shift in selectivity based on the nature of the promoter ions [26]. Many of these reactions have been reported by Vayenas et al [22]. Common examples are methane oxidation [42], ethylene oxidation [25], *NO* reduction by *CO* and  $C_3H_6$  [26], *CO* oxidation [24],  $CO_2$  hydrogenation [43]. The reactions were modified using different kinds of promoters, both of anionic and cationic nature. Accordingly, the catalyst material and the electrolytes were also varied.

The improvement in reaction rate in majority of the reactions shows that *EPOC* phenomenon is not specific to a particular type of reaction or an electrode-electrolyte system [21]. Rather, it is a generic concept. The subsequent sections deal with the theoretical understanding of the *EPOC* phenomenon in terms of thermodynamics, kinetics and the commonly used definitions in this field. It also includes previously done work on understanding the theoretical basis of this phenomenon.

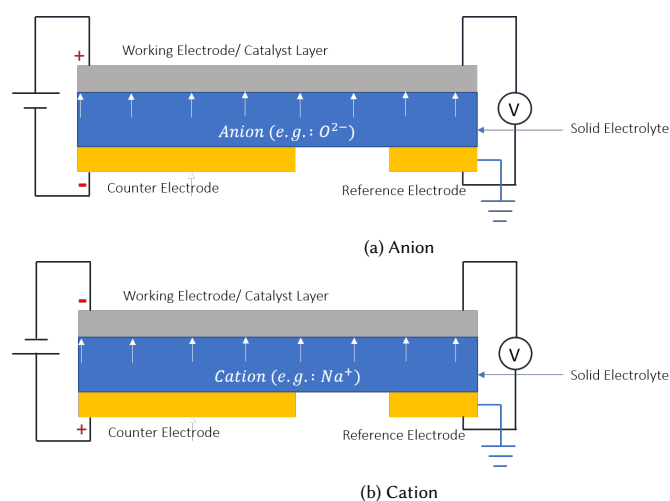
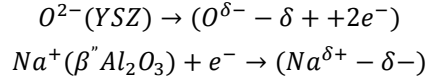


Figure 2.1: Anionic and Cationic transport of ions to the catalyst surface.

### 2.1.1 Thermodynamics

Efforts on understanding from the theoretical perspective were made by several groups in the past. *Brosda* and *Vayenas* explained the general theory based on electrostatics [23]. It included the effect of double layer formed over the catalyst surface which modifies the adsorption of the reactants, desorption of products and surface reactions. Figure: 2.1 shows the transport of the ions from the electrolyte to the catalyst surface. It includes the cases for both anion and cation. Anions move towards the catalyst when it is positively polarised and cations move towards it when it is negatively polarised.

There is a strong effect of electrostatics in *EPOC* [22]. The back-spillover ions on the catalyst surface form an electrically neutral double layer (e.g.,  $Na^{\delta+} - \delta^-$ ). Reactions taking place for  $O^{2-}$  and  $Na^+$  ions as promoters on reaching the catalyst surface are shown below [21].



Apart from these reactions, the ions may also get consumed at the triple phase boundary between the catalyst, electrolyte and the gas phase. For example, in case of  $O^{2-}$ ,  $O_2$  molecules might form or even  $O^{2-}$  ion can react with the reactants of the given heterogeneous reaction [21]. The metal surface develops equal and opposite charge to that of the ions to induce electroneutrality. Effectively, this leads to the formation of dipoles on the catalyst surface [22]. Figure: 2.2 shows the back-spillover of  $Na^+$  ions on the catalyst surface. The generated electric field changes the work function of the catalyst [22]. Such a modification has an impact on the activation energy of the reactant molecules. It weakens the bond strength of certain molecules on the catalyst surface whereas it is strengthened for the others [23]. Depending on the operating conditions, the overall reaction rate can increase tremendously compared to its original reaction rate for the same active catalyst area. The reaction takes place at a much higher rate than that of the electrochemically generated promoter ions [21]. Thus, the process is not faradaic and hence, the name non-faradaic electrochemical modification of catalytic activity.

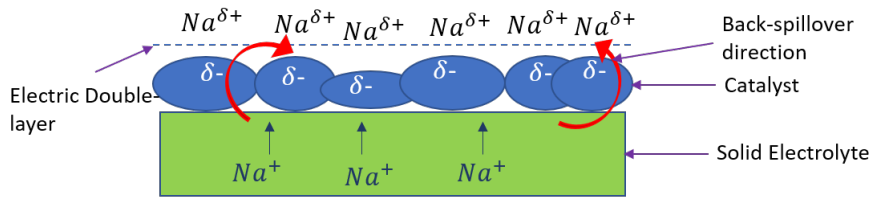


Figure 2.2: Back-spillover of  $Na^+$  ions on the catalyst surface.

*Vayenas* and *Tsiplakides* [44] has stated that the change in work function is approximately proportional to the change in the catalyst potential relative to the reference electrode. *Metcalfe* also showed from thermodynamic considerations that the change in work function of the catalyst is equivalent to the overpotentials on the catalyst surface [45]. *Leiva* considered position dependent electric field and by solving the Poisson's equation, concluded that there is a linear relationship between work function and applied overpotential [46]. Even calculations using rigorous quantum mechanical theory showed similar behaviour [47]. Equation: 2.1 shows the relationship between the change in the work function and the applied overpotential [44].

$$\Delta\phi = e \cdot \Delta V_{WR} \quad (2.1)$$

Equation: 2.1 is valid only when the transfer of the promoter ions is faster than their desorption or catalytic consumption. Otherwise deviations can be observed from this equation. A more generalised equation is shown below: [22]

$$e \cdot \Delta V_{WR} = \Delta\phi + \Delta\psi \quad (2.2)$$

where,

$$\Delta\psi = \text{Change in the outer Volta Potential of the metal catalyst, [eV]}$$

$\Delta\psi$  is equal to zero when there is no net surface charge available on the metal, i.e., the case in the presence of the electrically neutral double layer.

The change in work function modifies the enthalpy of the adsorbates. The change in the enthalpy as a function of the change in work-function is shown mathematically by equation: 2.3 [22]. It is calculated based on the assumption that only electrostatic effect is responsible for the modifications.

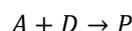
$$\Delta H = \lambda_j \cdot \Delta\varphi \quad (2.3)$$

where,

$$\begin{aligned} \lambda_j &= \text{Charge transfer coefficient of species } j \\ \Delta\varphi &= \text{Change in work function} \end{aligned}$$

### 2.1.2 Promotional Rules

There are four main types of reactions based on the adsorption strength of different reacting molecules [22]. For simplicity, a reaction consisting of an acceptor and a donor is considered and assuming, the following reaction takes place:



Here,  $A$  stands for acceptor,  $D$  stands for donor and  $P$  stands for Product.

#### a) Electrophobic Reaction

An electrophobic reaction is the one whose kinetics are in positive order for donor and negative or zero order for acceptor. The reaction rate for such reactions increases with increase in work function ( $\varphi$ ) or applied potential as shown in equation: 2.4 [22]. This is also depicted in fig: 2.3. Alternatively, it can be stated that if  $k_A \cdot P_A \gg 1$  and  $k_A \cdot P_A \gg k_D P_D$ , [22] the reaction is called electrophobic.  $k_A$  and  $k_D$  are the adsorption equilibrium constants for  $A$  and  $D$  respectively and  $P_A$  and  $P_D$  are their partial pressures. This means that the acceptor molecules strongly adsorb on the catalyst surface. Whereas, the donor atoms are weakly adsorbed to the catalyst surface.

$$\left(\frac{\partial r}{\partial \varphi}\right)_{P_A P_D} > 0 \quad (2.4)$$

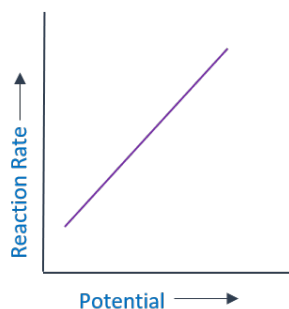


Figure 2.3: Electrophobic

#### b) Electrophilic Reaction

It is the exact reverse of the electrophobic reaction. Here, the kinetics of the acceptor molecule is positive order and for the donor molecule, it is negative or zero order. The reaction rate of electrophilic reactions decreases with increase in potential or work function ( $\varphi$ ) as shown in equation: 2.5 [22]. and fig: 2.4. It can also be said that if  $k_D \cdot P_D \gg 1$  and  $k_A \cdot P_A \ll k_D P_D$ , [22] then the reaction is called electrophilic. This means that the acceptor molecules weakly adsorb on the catalyst surface. Whereas, the donor atoms are strongly adsorbed to the catalyst surface.

$$\left(\frac{\partial r}{\partial \varphi}\right)_{P_A P_D} < 0 \quad (2.5)$$

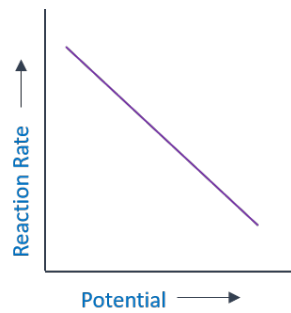


Figure 2.4: Electrophilic

## c) Volcanic Reaction

If both acceptor and donor are strongly adsorbed  $k_D \cdot P_D, k_A \cdot P_A \gg 1$  to the catalyst surface, then the type of the reaction is volcanic [22]. It is a combination of both electrophobic and electrophilic reactions. Initially, the reaction exhibits electrophobic behaviour which means increasing the voltage increases the reaction rate. It reaches a maximum and then starts decreasing with further increment in applied potential (electrophilic behaviour). Mathematically, it is described by equations: 2.6 [22]. Figure: 2.5 shows the variation in reaction rate with the applied potential.

$$\left(\frac{\partial r}{\partial \varphi}\right)_{P_A P_D} > 0, \varphi < \varphi_{max} \quad (2.6a)$$

$$\left(\frac{\partial r}{\partial \varphi}\right)_{P_A P_D} = 0, \varphi = \varphi_{max} \quad (2.6b)$$

$$\left(\frac{\partial r}{\partial \varphi}\right)_{P_A P_D} < 0, \varphi > \varphi_{max} \quad (2.6c)$$

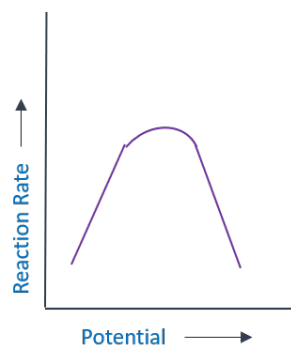


Figure 2.5: Volcano

## d) Inverted Volcanic Reaction

If both acceptor and donor are weakly adsorbed  $k_D \cdot P_D, k_A \cdot P_A \ll 1$  to the catalyst surface, then the reaction type is inverted volcanic type [22]. Initially, the reaction exhibits electrophilic behaviour. Thus, at first, increasing the voltage decreases the reaction rate. It reaches a minimum and then starts increasing with further increment in applied potential. Mathematically, it is described by equation: 2.7 [22]. The change in reaction rate with applied potential is depicted in fig: 2.6.

$$\left(\frac{\partial r}{\partial \varphi}\right)_{P_A P_D} < 0, \varphi < \varphi_{min} \quad (2.7a)$$

$$\left(\frac{\partial r}{\partial \varphi}\right)_{P_A P_D} = 0, \varphi = \varphi_{min} \quad (2.7b)$$

$$\left(\frac{\partial r}{\partial \varphi}\right)_{P_A P_D} > 0, \varphi > \varphi_{min} \quad (2.7c)$$

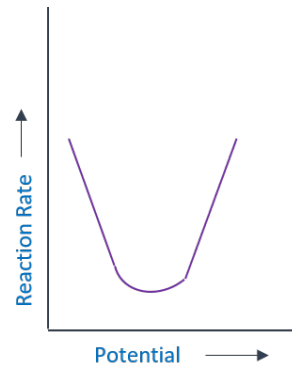


Figure 2.6: Inverted Volcano

Here,  $\varphi$  is the work function of the catalyst.  $\varphi_{max}$  is the work function at maximum reaction rate used in equations: 2.6 and  $\varphi_{min}$  is the work function at the minimum reaction rate which is shown in equations: 2.7.

### 2.1.3 Reaction Kinetics

Modifications in reaction rates due to *EPOC* can be modelled using different kinetic expressions. Existing models with modifications in adsorption, surface reaction and desorption can qualitatively or semi quantitatively capture the phenomenon [23]. *Brosda* and *Vayenas* extensively derived kinetic expressions based on *Langmuir Hinshelwood Hougen Watson (LHHW)* theory [23]. Expressions were derived for a series of hypothetical reactions ranging from monomolecular to bimolecular. Further, the kinetic expressions were tested for actual reactions like *CO* oxidation on Pt deposited on  $\beta'' - Al_2O_3$ . The experimental results and the modelling showed similar volcanic plot of reaction rate with respect to the catalyst potential [23]. *Metcalfe* [48] used transition state theory to predict the modified reaction rate and came to similar conclusion as *Brosda* and *Vayenas* [23]. *Brosda* and *Vayenas* also showed that other kinetic models like *Frumkin* or *Fowler Guggenheim* models are more complex and can land into mathematically intractable expressions [23]. Equations: 2.8 and 2.9 shown below provides the comparison between kinetic expressions for a general heterogenous reaction ( $A + D \rightarrow P$ ) with its electrochemically promoted counter part. These expressions are based on *LHHW* kinetics.

Heterogeneous [23]:

$$r^0 = k_r^0 \frac{k_A^0 P_A k_D^0 P_D}{(1 + k_A^0 P_A + k_D^0 P_D)^2} \quad (2.8)$$

where,

$$\begin{aligned} k_r^0 &= \text{Reaction rate constant} \\ P_{A/D} &= \text{Partial pressures of A and D} \\ k_{A/D}^0 &= \text{Rate constants for adsorption of A and D} \\ A &= \text{Acceptor} \\ D &= \text{Donor} \end{aligned}$$

Electrochemically Promoted [23]:

$$r = k_r^0 \exp(\lambda_r \Pi) \frac{k_A^0 P_A \exp(\lambda_A \Pi) k_D^0 P_D \exp(\lambda_D \Pi)}{(1 + k_A^0 P_A \exp(\lambda_A \Pi) + k_D^0 P_D \exp(\lambda_D \Pi))^2} \quad (2.9)$$

where,

$$\begin{aligned}\Pi &= \text{Non dimensional Potential} \\ \lambda_{A/D} &= \text{Charge transfer coefficient of A or D} \\ \lambda_r &= \text{Charge transfer coefficient of the transition state of the reaction}\end{aligned}$$

Non-dimensional potential  $\Pi$  can be calculated as follows:

$$\Pi = \frac{e\Delta V}{k_b T}$$

Equation: 2.9 is similar to equation: 2.8, except it has two additional terms,  $\exp(\lambda_A \Pi)$  and  $\exp(\lambda_D \Pi)$ . These are multiplied to the partial pressures of reactants  $A$  and  $D$  respectively to account for the change in their adsorption strength. Equation: 2.9 is valid for electrophobic, electrophilic and volcanic type of reactions. For inverted volcanic type, equation: 2.9 is modified as follows [23]:

$$r = k_r^0 \exp(\lambda_r \Pi) \frac{k_A^0 P_A \exp(\max(0, \lambda_A \Pi)) k_D^0 P_D \exp(\max(0, \lambda_D \Pi))}{1 + k_A^0 P_A \exp(\max(0, \lambda_A \Pi)) + k_D^0 P_D \exp(\max(0, \lambda_D \Pi))} \quad (2.10)$$

### 2.1.4 Commonly Used Terms

Terms common to the *EPOC* phenomenon are as follows:

**NEMCA Time Constant ( $\tau$ ):** It is the magnitude of time required for the reaction rate to reach 63 % of the maximum steady state value induced by *EPOC*. It is given by equation: 2.11b [21].

$$r = r_{max} (1 - \exp(-\frac{t}{\tau})) \quad (2.11a)$$

$$\tau = \frac{2N_G F}{I} \quad (2.11b)$$

**Faradaic Efficiency ( $\Lambda$ ):** Faradaic Efficiency or Enhancement factor is defined in equation: 2.12 [21]. It is the ratio of the change in the reaction rate due to *EPOC* and the rate of generation of promoter ions which follow the *Faraday's* law of electrolysis. In order to observe *EPOC* effect, Faradaic Efficiency should be greater than 1.

$$\Lambda = \frac{\Delta r}{\frac{I}{n F}} \quad (2.12)$$

Empirically, it was found that, Faradaic efficiency is dependent on the ratio of the unpromoted reaction rate and the faradaic generation of ions [21].

$$\Lambda \approx \frac{n F r_o}{I} \quad (2.13)$$

**Rate Enhancement Ratio ( $\rho$ ):** It is the ratio of reaction rate in promoted and that in unpromoted state. It is defined in equation: 2.14 [21].

$$\rho = \frac{r}{r_o} \quad (2.14)$$

**Promotional Index ( $PI_p$ ):** The promotional propensity of the promoter,  $PI_p$  can be quantified as in equation: 2.15. If this value is negative then the promoter ion is actually acting as a poison on the surface [21].

$$PI_p = \frac{\Delta r}{r_o \Delta \theta_p} \quad (2.15)$$

If  $PI_p > 0$ , then the ion acts as a promoter and on the other hand, if  $PI_p < 0$ , it is a poison for the reaction.

Nomenclature for the terms used in the above equations in this subsection: 2.1.4 are given below:

$$\begin{aligned}
 r &= \text{Reaction rate} \\
 r_{max} &= \text{Maximum steady state value of the reaction rate due to EPOC} \\
 N_G &= \text{Surface moles of catalyst, [moles/m}^2\text{]} \\
 F &= \text{Faraday's constant, [C/mol]} \\
 I &= \text{Current, [A]} \\
 \Delta r &= \text{Change in reaction rate} \\
 r_o &= \text{Reaction rate in the unpromoted state} \\
 n &= \text{Number of electrons shared during the generation of the promoter} \\
 \Delta\theta_p &= \text{Surface coverage of the promoter ions}
 \end{aligned}$$

### 2.1.5 Promoter Ions

Promoters are added to the catalyst in order to improve the activity, selectivity, stability and lifetime of the catalyst. Promotion of Ammonia synthesis using  $K$  on  $Fe$  catalyst is one of the examples, where promoters have been successfully used in commercial reactions [49].

Promoters are divided broadly into structural and electronic types [21]. As an example, ammonia synthesis on  $Fe$  catalyst can be considered again.  $Al_2O_3$  and  $K_2O$  are the two additives added to the  $Fe$  catalyst for ammonia synthesis.  $Al_2O_3$  acts as the structural promoter which improves the stability of the catalyst and increase the surface area of  $Fe$  by preventing crystal growth or agglomeration of  $Fe$  [21]. Whereas,  $K_2O$  offers electronic type of promotion due to the presence of  $K^+$  ions [21]. Promoters are known to modify the chemisorption properties of the co-adsorbed reactants. This can happen due to the interaction between the co-adsorbed reactants and the locally generated electric field [21].

Experiments on EPOC are commonly performed in solid state reactors where electrolytes are present to conduct the promoter ions to the catalyst surface. This is very similar to the SOFC reactors [21]. The choice of electrolyte materials depend on the promoter ion. This is because the electrolytes are selectively conductive to specific ions. Table: 2.1 shows the different promoter ions and their corresponding electrolytes.

Table 2.1: Promoter ions and their corresponding electrolyte materials

Promoters	Electrolytes	Ref
$Na^+$	$Na - \beta'' Al_2O_3$	[50]
$K^+$	$K - \beta'' Al_2O_3$	[51]
$O^{2-}$	YSZ	[52]
$H^+$	BZY	[41]

The type of promoter, anionic or cationic will have different effects to a reaction. If the reaction is electrophobic, then increasing the anion concentration on the catalyst surface will increase the productivity and similarly decreasing the cation concentration on the catalyst surface will also increase the productivity. This happens because electrophobic reactions show an increasing reaction rate with an increase in positive potential [22]. Exactly the opposite is valid for electrophilic reactions, i.e., electrophilic reactions show an decreasing reaction rate with increasing potential [22].

### 2.1.6 EPOC, Classical Promotion and Metal Support Interaction

Metal Support Interaction (MSI) takes place when a porous metallic support layer helps to stabilise the dispersed catalyst. The type of support will influence the activity and selectivity of the catalyst. In certain types of MSI, promotion takes place due to the migration of ionic species over the catalyst particles. For example in  $ZrO_2$ ,  $TiO_2$  and  $CeO_2$  based supports, the back-spillover of  $O^{2-}$  ions is similar to the case of EPOC or NEMCA using YSZ as the  $O^{2-}$  conducting electrolyte [21].

There is no functional difference between classical promotion and *EPOC* or even with *MSI* [21]. Both *EPOC* and *MSI* can promote the catalytic activity by the back-spillover of the promoter ions over the catalyst surface. Similarly, passing *Na* vapour over the catalyst layer in classical promotion will do the same work as in back-spillover of  $Na^+$  ions in *EPOC* [22]. Therefore, the difference among the three is not functional, but operational. Unlike the other two cases, in *EPOC* experiments, it is possible to accurately measure the spillover-backspillover rates. This is because the coverage of the promoters can be directly related to the magnitude of applied potential or current. Also the coverage of the promoters on the catalyst surface can be controlled through the application of electric current or potential [21].

Unlike classical promotion, *EPOC* has no limitation on the shorter lifetime of the promoter ions on the catalyst surface. This is because of the possibility of continuous replenishment of the promoter ions on the catalyst surface [22].

### 2.1.7 Effect of *EPOC* on different reactions

Table: 2.2 and 2.3 shows different reactions on which the effect of *EPOC* has been tested using *YSZ* and  $Na\beta''Al_2O_3$  as electrolytes respectively [22]. It includes the *Faradaic* efficiency ( $\Lambda$ ), rate enhancement ratio ( $\rho$ ) and promotional index ( $PI_p$ ) values.

Table 2.2: Reactions performed using *YSZ* electrolyte and  $O^{2-}$  promoter ion

Donor	Acceptor	Product	Catalyst	$\Lambda$	$\rho$	$PI_p$	Ref
$C_2H_4$	$O_2$	$CO_2$	<i>Pt</i>	$3 \cdot 10^5$	55	55	[53]
$C_2H_6$	$O_2$	$CO_2$	<i>Pt</i>	300	20	20	[54]
$CH_4$	$O_2$	$CO_2$	<i>Pt</i>	5	70	70	[55]
$C_2H_4$	$O_2$	$CO_2$	<i>Rh</i>	$5 \cdot 10^4$	90	90	[56]
$H_2$	$CO_2$	$CH_4, CO$	<i>Rh</i>	200	3	2	[21]
$CH_3OH$	$O_2$	$H_2CO, CO_2$	<i>Ag</i>	-95	2	-	[57]
$CH_4$	$H_2O$	$CO, CO_2$	<i>Ni</i>	12	2	-	[58]
$CO$	$N_2O$	$CO_2, N_2$	<i>Pd</i>	-20	2	-	[59]

Table 2.3: Reactions performed using  $\beta''Al_2O_3$  electrolyte and  $Na^+$  promoter ion

Donor	Acceptor	Product	Catalyst	$\Lambda$	$\rho$	$PI_p$	Ref
$C_2H_4$	$O_2$	$CO_2$	<i>Pt</i>	$5 \cdot 10^4$	0.25	-30	[60]
$CO$	$NO$	$CO_2, N_2, N_2O$	<i>Pt</i>	-	13	200	[26]
$H_2$	$NO$	$N_2, N_2O$	<i>Pt</i>	-	30	6000	[61]
$C_2H_4$	$O_2$	$C_2H_4O, CO_2$	<i>Ag</i>	-	-	40	[62]
$CO$	$O_2$	$CO_2$	<i>Ag</i>	-	2	-	[21]

In tables: 2.2 and 2.3, Donor and Acceptor stands for the reactants.

### 2.1.8 *EPOC* in Hydrogenation Reaction

$CO_2$  and  $CO$  hydrogenation are important as they hold the potential of producing hydrocarbons essential for many chemical industries. Hydrogenation reactions like Fischer Tropsch will become more and more important as the fossil based sources are depleting at an accelerating rate [10]. This is because *FT* uses  $CO$  and  $H_2$  as raw materials which can be obtained through electrolysis of  $CO_2$  and  $H_2O$  [63] or biomass gassification [64].

*FT* reaction is known to produce a wide distribution of products of different carbon lengths. It is desirable to have a higher selectivity towards a narrower product range. In such a case, *EPOC* can have the potential to modify the productivity and selectivity under appropriate operating conditions.

Apart from *FT*, other hydrogenation reactions of interest are  $CO_2$  hydrogenation to  $CH_4$  [65],  $CO_2$  to  $C_2 - C_5$

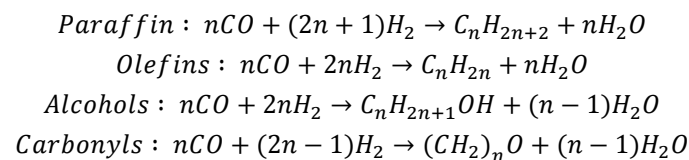
[66], acetylene hydrogenation to  $C_2H_4$  and  $C_2H_6$  [67]. Makri et al conducted experiments on  $CO_2$  hydrogenation on nano-dispersed 2%  $Ru/YSZ$  catalysts [68]. In this work, conversion of  $CO_2$  to  $CH_4$  showed electrophobic behaviour, whereas conversion towards  $CO$  showed electrophilic behaviour. With increasing potential,  $O^{2-}$  concentration increases on the catalyst surface. Hence, rate of production of  $CH_4$  increases and that of  $CO$  drops.

*Kotsiras et al* investigated  $CO_2$  hydrogenation on nano dispersed  $Ru - Co$  catalyst deposited on a  $Ru$  film on  $BZY$  electrolyte [65]. They showed increase in  $H^+$  concentration increases  $CO$  concentration. *Grigoriou et al* have reported formation of hydrocarbons up to  $C_5$  on 2%  $Ru - 15\% Co/BZY$ , even though the maximum yield was less than 0.3% [66]. They stated that with increasing concentration of  $H^+$ ,  $Ru$  nanoparticles produced  $CO$  which reacted into higher hydrocarbons on  $Co$  nano particles via  $FT$  reaction.

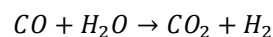
## 2.2 Fischer Tropsch Reaction

$FT$  synthesis is a catalytic polymerisation process to convert  $CO$  and  $H_2$  into hydrocarbons. It was first developed by *Franz Fischer* and *Hanz Tropsch* in Germany, 1925 [69]. It is operated at high temperature of around 150 – 300°C [70] and pressure of about 20 – 30 bar [71]. In the recent decades, Fischer Tropsch reaction has become a topic of interest among the researchers as it holds the potential of producing liquid fuels [72]. This can be an alternative to the traditional ways like production of liquid fuels from oil reserves [10] [72]. Such an alternative is necessary because of the limited oil reserves and their continuous depletion [10].

$FT$  uses  $CO$  and  $H_2$  as raw materials.  $CO$  is traditionally produced from coal, natural gas or biomass via gasification process [64]. This synthesis gas is further used in the  $FT$  reaction which leads to the formation of liquid hydrocarbons (Gas to liquid process).  $FT$  involves the formation of monomeric units which are polymerised to a wide distribution of products. It includes paraffins, olefins alcohols and carbonyls [10]. Also, a wide spectrum of carbon lengths can be observed on the products. Depending on the operating and inlet conditions, different kinds of products can be obtained. Following are the general reactions taking place in the process [10], [73]:



Other side reactions like Water Gas Shift reaction can also take place [73].



$FT$  reactions have been studied on various catalysts which include,  $Fe$ ,  $Co$ ,  $Ru$ ,  $Rh$ , etc. Out of these,  $Fe$  and  $Co$  have found industrial usage.  $Ru$  is known to produce longer hydrocarbon chains, it is highly expensive, almost about 50,000 times more than  $Fe$  [70]. Cobalt is about 230 times more expensive than iron, but its operating cost is lower and has a longer lifetime<sup>1</sup>. This is because of its resilience towards coke deposition [10]. It also inhibits the formation of  $CO_2$  via water gas reaction [74]. Linear alkanes are the major products on  $Co$  catalyst.

### 2.2.1 Reaction Kinetics

$FT$  reaction involves complex kinetics due to the formation of a wide range of products. Different expressions have been developed by various groups based on their experimental observation and theoretical analysis. Many of them are based on Langmuir Hinshelwood kinetics [75]. The variations depend on the type of catalysts. A simpler first order kinetics was developed by *Post et al* as shown in equation: 2.16 [76]. It is a function of

<sup>1</sup><https://www.netl.doe.gov/research/coal/energy-systems/gasification/gasifipedia/ftsynthesis>

only the  $H_2$  concentration ( $C_{H_2}$ ). While this has been used in many reactor models, the authenticity of the expression can be shown only for smaller CO conversion, i.e., CO conversion <60% [71].

$$r = k_o \exp\left(\frac{-E_a}{RT}\right) C_{H_2} \quad (2.16)$$

Table 2.4: Parameters used in *Post et al* expression:2.16

Parameters	Values
$k_o$	$3.107 \cdot 10^{10} [m^3 \cdot m_{cat}^{-3} \cdot s^{-1}]$
$E_a$	$120 [kJ/mol]$

A more realistic expression was developed by *Yates and Satterfield* based on *Langmuir – Hinshelwood* kinetics [77]. Equation: 2.17 is valid in higher conversion range. It is a function of the partial pressures of both CO and  $H_2$ .

$$r = \frac{a P_{CO} P_{H_2}}{(1 + b P_{CO})^2} \quad (2.17)$$

Here,

$$a = a_0 \exp\left(\frac{\Delta E_a}{R T} \left(\frac{1}{493.15}\right) - \frac{1}{T}\right)$$

$$b = b_0 \exp\left(\frac{\Delta H}{R T} \left(\frac{1}{493.15}\right) - \frac{1}{T}\right)$$

Table 2.5: Parameters used in *Yates and Satterfield* expression:2.17

Parameters	Values
$a_0$	$8.88533 \cdot 10^{-3} [mol \cdot s^{-1} \cdot kg_{cat}^{-1} \cdot bar^{-2}]$
$b_0$	$2.226 [bar^{-1}]$
$\Delta E_a$	$3.737 \cdot 10^4 [J \cdot mol^{-1}]$
$\Delta H$	$-6.837 \cdot 10^3 [J \cdot mol^{-1}]$

*Iglesia et al* derived a similar expression as shown in equation [78]. The values of  $a$ ,  $b$  and  $k_i$  depends on the catalyst material and also the reaction. They used Co and Ru catalyst for the study.

$$r = \frac{k_i C_{CO}^a C_{H_2}^b}{1 + K C_{CO}} \quad (2.18)$$

The values of the constants  $k_i$ ,  $a$ ,  $b$  and  $K$  are shown in 2.6 [78]. The units of these constants are formulated in such a way that the reaction rate unit is *moles/(g – atom surface metal · s)* with reaction orders  $a$  and  $b$ .

Table 2.6: Parameters used in expression:2.18

Parameters	Cobalt	Ruthenium
$k_i$	$1.96 \cdot 10^{-8}$	$7.46 \cdot 10^{-11}$
$K$	$3.33 \cdot 10^{-5}$	$3.33 \cdot 10^{-5}$
$a$	0.6	1.0
$b$	0.65	0.6

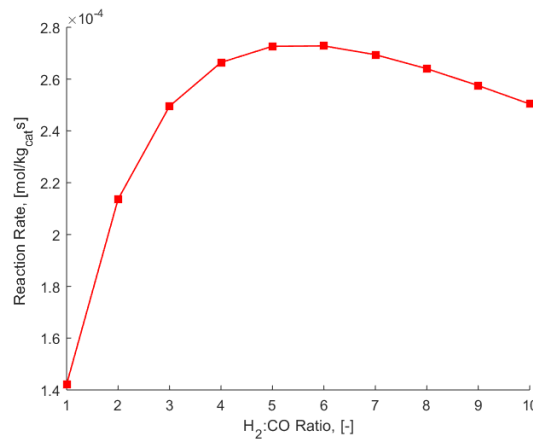


Figure 2.7: Variation of reaction rate with  $H_2 : CO$  ratio.

Among these expressions, the one proposed by *Yates* and *Satterfield* (equation:2.17) is commonly used and therefore, it has been used in this thesis too. Figure: 2.7 shows the effect of variation on the ratio of Partial pressures ( $H_2 : CO$ ) on the reaction rate. Equation: 2.17 has been used to study the trend. Initially, fig: 2.7 shows an increasing trend for the reaction rate with higher  $H_2 : CO$  ratio. After reaching a maximum, the magnitude of rate starts lowering.

## 2.2.2 Product Distribution

As already mentioned, *FT* leads to a broad distribution of products. Anderson developed a model from the one proposed by Schultz and Flory for polymerisation reaction which is shown in equation: 2.19 [79]. The Weight fraction is a function of the chain growth probability ( $\alpha$ ) and carbon number ( $n$ ).

$$w = \alpha^{n-1} \cdot n \cdot (1 - \alpha)^2 \quad (2.19)$$

The chain growth probability factor which can be calculated as shown by equation: 2.20 [80]. Higher the value of chain growth probability factor, greater is the chance of producing longer carbon chains. It depends on feed composition, catalyst material and design and operating temperature [10].

$$\alpha = \left( A \cdot \frac{P_{CO}}{P_{CO} + P_{H_2}} + B \right) (1 - C \cdot (T - 533)) \quad (2.20)$$

where,

$$A = 0.2332 \pm 0.0420$$

$$B = 0.6330 \pm 0.0420$$

$$C = 0.0039$$

$$P_i = \text{Partial pressure of reactant } i$$

$$T = \text{Temperature}$$

*Schultz-Flory* expression is widely used to model the product distribution of *FT* reaction, although quite a significant deviations could be observed from real experiments especially for the weight fractions of  $C_1$  and  $C_2$  [75]. Significantly large amount of methane is generated in experiments. Deviations of weight fractions of other carbon molecules from equation: 2.19 might occur because Schultz and Flory distribution does not consider olefin re-adsorption [81].

## 2.2.3 Effect of Temperature

Narrowing down the wide distribution of products is one of the major challenges while using *FT*. It depends a lot on the operating conditions (Temperature and Pressure), the type of catalyst, mass transfer characteristics, etc [12]. There are two operating ranges of temperature [70]:-

1. Low Temperature FT: (200 – 270°C) Longer Carbon chains can be achieved in this temperature range.
2. High Temperature FT: (300 – 350°C) Higher temperature leads to faster conversion but in this range low  $C_n$  are formed.

Figure: 2.8 shows the variation of weight fraction for carbon numbers at different temperatures. It is calculated using the Schultz Flory distribution described by equation: 2.19. Fig: 2.8 shows that higher the temperature, weight fractions of shorter carbon lengths increase. At lower temperature, longer carbon chains and broader product distribution are formed.

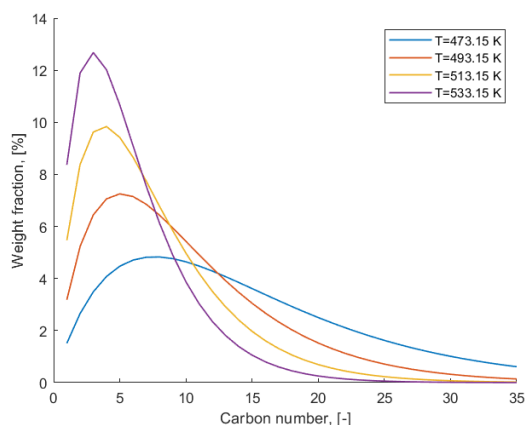


Figure 2.8: Weight fraction of FT products at different temperatures.

## 2.2.4 Effect of Alkali Promotion

Alkali promotion improves the  $CO$  adsorption and dissociation and inhibits  $H_2$  adsorption [82], [83]. Improvement in  $CO$  dissociation increases the carbon atom concentration on the catalyst surface, thus, increasing the chain growth probability. Again, inhibition of  $H_2$  adsorption reduces the probability of hydrogenation [82]. Hence, selectivity of olefins over paraffins increases. This is because olefins are produced by dehydrogenation process whereas, paraffins are produced by hydrogenation.

*Okuhara et al* studied the role of *Potassium*, *Boron* and *Phosphorous* on  $CO$  hydrogenation over Alumina supported *Ru* [82]. They have found that *Potassium* improved *olefin – paraffin* ratio and suppressed methane formation but decreased overall catalytic activity. Whereas, *Boron* and *Phosphorous* showed opposite behaviour [82].

Similar results were also obtained when alkali promotion was done electrochemically instead of classical manner. *Williams* and *Lambert* experimentally studied the effect of sodium promotion on FT over *Ru* catalyst [50]. They reported enhancement in chain growth probability with increase in  $Na^+$  concentration over the catalyst surface. *Olefin – paraffin* ratio was improved with decreasing potential or equivalently increasing  $Na^+$  coverage. They also concluded an overall decrease in the reaction rate with increase in  $Na^+$  concentration. *Urquhart et al* studied the electrochemical promotion of FTS on *Rhodium* catalyst using  $K^+$  ions [51], [84]. They have found that Alkali promotion increases  $C_2 – C_4$  selectivity at atmospheric pressure but reduced overall activity or production rate [84]. At higher pressure they could observe enhancement in selectivity for alkenes and linear alcohols [51]. Similar conclusions were made about reaction rate which decreased with increase of promoter ion concentration.

## 2.2.5 Periodic Operation in Fischer Tropsch

Periodic Operation in FT has been studied by varying the concentration of the feed [85], [86] and the operating temperature [87]. Modulation of the feed ratio has been the common method to study the periodic

operation on *FT*. *Nicopoulos et al* have studied the effect of  $H_2$  pulsing on the activity and product distributions [85]. They used  $\alpha - Co/ZrO_2/SO_2$  as a catalyst.  $H_2$  pulsing lead to higher  $CO$  convergence but gradually decreased to the steady state until the next pulse occurred. With the  $H_2$  pulsing, an increase in the yield of  $CH_4$  and  $C_{10} - C_{20}$  have been reported by the author compared to the steady state operation [85]. Study of hydrocarbon rate formation using cobalt oxide as the catalyst and forced cycling of concentration feed was done by *Adesina et al* [86]. They found that along with higher methane production, there was rate enhancement for  $C_2$  to  $C_6$  molecules. This suggested that periodic operation can hold the potential of tuning the selectivity of the *FT* reaction [86].

*Dautzenberg et al* investigated the effect of forced cycling with equimolar mixture of  $CO$  and  $H_2$ , in an otherwise pure  $H_2$  feed [87].  $Ru - \gamma Al_2O_3$  was used as the catalyst. Along with the feed the temperature was also varied. In the carbon rich regime, the temperature is  $210^\circ C$  and in the pure  $H_2$  regime it is increased from  $210^\circ C$  to  $350^\circ C$ . This was done to enforce chain termination and product desorption [87]. Unlike the steady state, a narrow product distribution was reported and with increasing the carbon rich regime, probability of the growth of longer carbon chain is increased [87].

*Ruthenium* and *Cobalt* based catalysts were positively influenced by the periodic operation [88], [89]. These catalysts showed improvement in the rate of formation and selectivity of the reaction. However, not always positive effect have been observed. Periodic operation with hydrogen pulsing on supported iron catalyst showed sharp increase in methane formation and hardly any increase in  $C_{2+}$  products [90]. As mentioned above, influence of periodic change in feed concentration on *FT* has been majorly studied in the past. But no work on periodic application of *EPOC* phenomenon on *FT* reaction has been found in the literature. The influence of this phenomenon will be studied as a part of this work.



## Chapter 3

# Modelling

The first part of the study begins with the relationship between surface promoter coverage with the applied potential or the work function of the catalyst. It also involves the application of analytical or semi-empirical expressions to study the effect of *EPOC* on *FT*. These expressions are used to study the effect of the applied potential on the chain growth probability, reaction rate and olefin-paraffin ratio. Although, the expressions have been adopted from literature, they had to be modified to take into account the *EPOC* effect. The changes were made to capture the variations in adsorption of the reactant molecules due to the double layer effect of *EPOC*. The equations are explained with necessary derivations in section: 3.2. Further, the same equations were used to study the combined effect of operating conditions (*temperature*,  $H_2 : CO$  feed ratio and *pressure*) and *EPOC*. Additionally, a *CSTR* plug flow reactor model has been used to study the effect of pressure on the conversion of the reactants. This *CSTR* model can also show the temporal variations of different products formed during the *FT* reaction. Formation of olefins and paraffins at a given potential can be distinguished using this model.

For the dynamic or periodic *EPOC* case, it is vital to calculate the time scale required for the ions to reach the top surface of the catalyst from the electrolyte. For that, one dimensional diffusion equation is solved for the transport of the concerned ions. This equation can calculate the surface coverage of ions at different times.

To study the periodic application of *EPOC* on *FT* reaction, again, *CSTR* plug flow model has been assumed. Here, the reaction rates for the products are not based on the *Anderson Schulz Flory (ASF)* model. The reason for this is explained in section: 3.3. The periodicity is studied here in the form of a square wave. Effects of frequency, symmetry of the periodic wave or its duty cycle and the amplitude of the wave on *FT* process are investigated.

For the study of reactor design, an *SOFc* type reactor is chosen. Steady state one dimensional species and energy balance equations are modelled to calculate the conversion of reactants and temperature variation along the length of the reactor. Finally, these results are used to understand the opportunities and difficulties in scaling up of *FT* reactors with *EPOC* effect.

### 3.1 Surface Coverage of Promoter Ions

Understanding the dependence of surface coverage of ions on the applied potential is important because that will finally modify the activity and / or selectivity of the given reaction. The coverage of the promoter ions can be related to the work function of the catalyst using *Helmholtz* equation [91]. This is shown in equation: 3.1. Equations: 3.1a and 3.1b show the relationship of the surface coverage with the change in work function and applied potential respectively.

$$\Delta\varphi = \frac{eN_m}{\epsilon_o} \cdot P_j \cdot \Delta\theta \quad (3.1a)$$

$$\Delta V = \frac{N_m}{\epsilon_o} \cdot P_j \cdot \Delta\theta \quad (3.1b)$$

where,

$$\begin{aligned}\Delta\phi &= \text{Change in work function, [J]} \\ N_m &= \text{Surface atomic density, [atoms/m}^2\text{]} \\ P_j &= \text{Dipole Moment, [C m]} \\ \Delta\theta &= \text{Change in surface coverage, [-]} \\ \Delta V &= \text{Change in applied potential, [Volt]}\end{aligned}$$

## 3.2 EPOC in Fischer Tropsch

Initially the effect of *EPOC* on Fischer Tropsch reaction has been studied through zero dimensional model. Analytical and semi empirical equations that are commonly used to study the *FT* process are used here. Chain growth probability and reaction rate are modified to accommodate the effect of *EPOC*. The changes due to *EPOC* can take place in the adsorption, surface reaction and desorption [22]. In this study, changes in the adsorption of *CO* and *H<sub>2</sub>* have been taken into account. *Brosda* and *Vayenas* stated that this can be done by changing the partial pressure or the activity term of the reactants [23]. This is shown by equations: 3.5a and 3.5b. Also, a derivation has been made for calculating the *olefin – paraffin* ratio based on the changes in the desorption of the olefins and paraffins. This is shown in sub-section: 3.2.4. Only olefins and *n*-paraffins are considered as the products and carbide mechanism with *CO* and *H<sub>2</sub>* dissociation [92] have been assumed.

Before diving into the the derivations of the equations for *FT*, it is important to understand the concept of charge transfer coefficient.

### 3.2.1 Charge Transfer Coefficient

It quantitatively describes the electronic interaction between the molecules and the catalyst surface. Larger is the magnitude of this coefficient, higher is the interaction with the surface. Charge transfer interactions between molecules and the catalyst surface take place when the electronic structure of the surface of the catalyst is modified. This can happen due to the existence of ions on the catalyst surface. Presence of cations makes the surface negatively charged and anions make it positively charged. Such separation of charges lead to dipole interaction and becomes responsible for changing the work function of the catalyst surface [44].

This modification will have an effect on the adsorption and desorption of reactants and products respectively. Electrophilic molecules will be attracted towards electron rich surface and electrophobic molecules will be attracted towards electron deficient surface [44].

The magnitude of charge transfer coefficient depends on the extent of the electronic interaction. In many cases in electrochemical reactions, the value is approximately  $\pm 0.5$ . In case of *EPOC*, the interaction is relatively weaker as the reaction is still heterogeneous rather than electrochemical. Possible values of  $\lambda$  could be in between  $-0.15$  and  $0.15$  approximately [23].

The study deals with *FT* reaction in which the two reactants are *CO* and *H<sub>2</sub>*. *CO* is electrophilic and *H<sub>2</sub>* is electrophobic in nature. If cationic promoters are added, *CO* will be strongly adsorbed on the surface. If anionic promoter is added, *H<sub>2</sub>* will be strongly adsorbed. The changes in the adsorption of reactants dictate the selectivity and reactivity of the reaction.

In this work, charge transfer coefficients for *CO* and *H<sub>2</sub>* are assumed to be  $-0.05$  and  $0.05$  respectively. Sign conventions are as per stated by *Vayenas et al* [23]. Negative sign in charge transfer coefficient denotes that the molecule is electron acceptor and positive sign denotes that it is electron donor. There could be also changes in the transition states of the elementary reactions due to the presence of the ions on the catalyst surface. But such complexities are avoided here as it is difficult to calculate or even find experimental data on the charge transfer coefficients for the transition states. Even without including such effects, a good qualitative picture can be drawn [23].

Following subsections describe the modifications made to the existing equations in the study of Fischer Tropsch.

### 3.2.2 Chain Growth Probability

Chain Growth Probability tells about the product distribution of the reaction. Higher its value, greater is the chain length of the hydrocarbons produced. Mathematically, it can be defined as the ratio of rate of propagation to the sum of rates of propagation and termination which is represented by eq: 3.2 [93].

$$\alpha = \frac{r_p}{r_p + r_t} \quad (3.2)$$

Here,  $r_p$  is the rate of production and  $r_t$  is the rate of termination.

Chain Growth Probability value depends on various factors like temperature, feed composition ( $H_2 : CO$  ratio) and catalyst promoter level [10]. Different semi-empirical expressions have been developed to predict the chain growth probability. Equation: 3.3 shows one developed by Song *et al* [80].

$$\alpha = (A \cdot \frac{P_{CO}}{P_{CO} + P_{H_2}} + B)(1 - C \cdot (T - 533)) \quad (3.3)$$

where,

$A, B$  and  $C = \text{Constants}$

$P_i = \text{Partial pressure of reactant } i$

$T = \text{Temperature}$

Vervloet *et al* also derived an expression for chain growth probability based on the propagation and termination rate constants and  $H_2 : CO$  ratio which is shown in equation:3.4 [93].

$$\alpha = \frac{1}{1 + k_\alpha \cdot (\frac{C_{H_2}}{C_{CO}})^\beta \cdot \exp(\frac{\Delta E_\alpha}{R} \cdot (\frac{1}{493.15} - \frac{1}{T}))} \quad (3.4)$$

where,

$k_\alpha = \text{Ratio of rate constants for propagation and termination reactions}$

$\beta = \text{Syngas ratio power constant}$

$\Delta E_\alpha = \text{Difference in activation energy for propagation and termination reactions}$

The above equations 3.3 and 3.4 can be modified to capture the effect of the promoter ions or the applied potential. For that, the partial pressures or the concentrations are modified as follows.

$$P_i = P_i^0 \cdot \exp(\lambda_i \cdot \frac{e\Delta V}{k_b T}) \quad (3.5a)$$

$$C_i = C_i^0 \cdot \exp(\lambda_i \cdot \frac{e\Delta V}{k_b T}) \quad (3.5b)$$

where,

$P_i = \text{Partial Pressure of reactant } i$

$C_i = \text{Concentration of reactant } i$

$\lambda_i = \text{Charge transfer coefficient of } i$

$i = CO \text{ or } H_2$

$\Delta V = \text{Change in the catalyst potential wrt a reference potential at which promoter ion coverage is zero}$

Equations: 3.5a and 3.5b take into account the change in adsorption of the reactants due to the interfacial potential. Accordingly, eq: 3.5a can be used in eq: 3.3 which gives

$$\alpha = (A \cdot \frac{P_{CO} \cdot \exp(\lambda_{CO} \cdot \frac{e\Delta V}{k_b T})}{P_{CO} \cdot \exp(\lambda_{CO} \cdot \frac{e\Delta V}{k_b T}) + P_{H_2} \cdot \exp(\lambda_{H_2} \cdot \frac{e\Delta V}{k_b T})} + B)(1 - C \cdot (T - 533)) \quad (3.6)$$

The values of the constants  $A$ ,  $B$  and  $C$  are obtained by fitting the equation: 3.6 to the experimental data provided by *Williams and Lambert* on *MATLAB* using *fminsearch* function [50]. These are listed below in table: 3.1.

Table 3.1: Constants for equation:3.6

Constants	Values
$A$	0.0226
$B$	0.0337
$C$	0.1050

Similarly, using eq: 3.5b, eq: 3.4 can be modified as:

$$\alpha = \frac{1}{1 + k_\alpha \cdot \left( \frac{C_{H_2} \cdot \exp(\lambda_{H_2} \cdot \frac{e\Delta V}{k_b T})}{C_{CO} \cdot \exp(\lambda_{CO} \cdot \frac{e\Delta V}{k_b T})} \right)^\beta \cdot \frac{\Delta E_\alpha}{R} \cdot \left( \frac{1}{493.15} - \frac{1}{T} \right)} \quad (3.7)$$

The fitted parameters are shown below in table: 3.2

Table 3.2: Constants for equation:3.7

Constants	Values
$k_\alpha$	0.59, [-]
$\beta$	0.176, [-]
$\Delta E_\alpha$	120, [kJ/mol]

The results drawn after fitting the equations: 3.6 and 3.7 with experimental data, are shown in fig:4.2a and 4.2b in Chapter: 4.

Chain growth probability ( $\alpha$ ) can be used to calculate the weight fraction or molar fraction for different products formed. *Anderson Schulz Flory (ASF)* expression is commonly used to describe the fractions. Equations: 3.8a and 3.8b are used to calculate the values of the weight fractions and mole fractions respectively for different lengths of carbon chains.

$$w_f = \alpha^{n-1} \cdot n \cdot (1 - \alpha)^2 \quad (3.8a)$$

$$m_f = \alpha^{n-1} \cdot (1 - \alpha)^2 \quad (3.8b)$$

### 3.2.3 Reaction Rate

Reaction rate for Fischer Tropsch reaction is a complex one as it involves large number of intermediates owing to its polymeric nature. It can vary from condition to condition and also due to the use of different types and morphology of the catalyst material. Catalyst material also dictates the reaction mechanism leading to different types of products. One of the most commonly used expression for studying *FT* reaction rate was proposed by *Yates and Satterfield* [77]. The reaction rate has been shown in Chapter: 2. The modified reaction rate has been shown here by equation: 3.9.

$$r = \frac{a \cdot P_{CO} \exp(\lambda_{CO} \cdot \frac{e\Delta V}{k_b T}) \cdot P_{H_2} \exp(\lambda_{H_2} \cdot \frac{e\Delta V}{k_b T})}{(1 + b \cdot P_{CO} \exp(\lambda_{CO} \cdot \frac{e\Delta V}{k_b T}))^2} \quad (3.9)$$

where,

$$a = a_o \cdot \exp\left(\frac{\Delta E_a}{R} \left(\frac{1}{493.15} - \frac{1}{T}\right)\right), \left[\frac{\text{mol}}{\text{s kg}_{cat} \text{ bar}^2}\right]$$

$$b = b_o \cdot \exp\left(\frac{\Delta H}{R} \left(\frac{1}{493.15} - \frac{1}{T}\right)\right), \left[\frac{1}{\text{bar}}\right]$$

Similar to the case of chain growth probability, partial pressures of  $CO$  and  $H_2$  have been modified to take into account the change in their adsorption strength. The values of  $a_o$  and  $b_o$  are modified according to the experiments of *Williams and Lambert* [50]. These are mentioned below in table: 3.3. The unit of the reaction rate is  $[\text{mol}/(\text{kg}_{cat} \text{ s})]$ .

Table 3.3: Constants for equation:3.9

Constants	Values
$a_o$	$1.18 \cdot 10^{-6}, [\text{mol}/(\text{s kg}_{cat} \text{ bar}^2)]$
$b_o$	$0.9643, [1/\text{bar}]$
$\Delta E_a$	$37.3665, [\text{kJ}/\text{mol}]$
$\Delta H$	$-68.4741, [\text{kJ}/\text{mol}]$

### 3.2.4 Olefin-Paraffin Ratio

Several studies on Fischer Tropsch reaction have shown that production of olefin decreases with increasing carbon number and found that olefin- paraffin ratio follows an exponential decay with carbon number. *Kuipers et al* [94] and *Iglesia et al* [81] have shown that *Olefin – Paraffin ratio*  $\sim \exp(-c \cdot n)$ . *Kuipers et al* have shown that the value of  $c$  comes from the physisorption energy of the olefin present on the catalyst surface [94]. *Todic et al* approximated that the rate of desorption of olefin depends on the carbon number whereas the rate of desorption for paraffin is independent of it [95].

It is important to note that paraffin formation takes place with the addition of adsorbed hydrogen to the  $\alpha$  position of the adsorbed carbon chain. Along with this, the effect of the applied potential or alkali coverage, also has to be taken into account. Olefin production may not experience a direct influence of the EPOC effect because olefins are formed by elimination of the  $\beta$  hydrogen. There is no interaction with adsorbed hydrogen. But paraffins do, as they involve the addition of adsorbed hydrogen to the  $\alpha$  position carbon. The effect of EPOC on the transition states have not been considered.

Taking these points into account and assuming the rate of production of olefins and paraffins are functions of the partial pressures of  $CO$  and  $H_2$  the following derivation gives an expression for the *Olefin – Paraffin* ratio.

$$r_o = k_o^0 \cdot P_{CO} \cdot \exp\left(-\frac{\Delta G_{phy}}{RT} \cdot n\right) \quad (3.10a)$$

$$r_p = k_p^0 \cdot P_{CO} \cdot P_{H_2} \exp\left(\lambda_{H_2} \frac{e\Delta V}{k_b T}\right) \quad (3.10b)$$

$$OP = \frac{r_o}{r_p}$$

$$OP = \frac{k_o^0}{k_p^0} \cdot P_{H_2}^{-1} \cdot \exp\left(-\frac{\Delta G_{phy}}{RT} \cdot n\right) \cdot \exp\left(-\lambda_{H_2} \frac{e\Delta V}{k_b T}\right) \quad (3.10c)$$

where,

$$\begin{aligned}
 r_o &= \text{Rate of production of olefins, [bar}^{-1}\text{s}^{-1}] \\
 r_p &= \text{Rate of production of paraffins, [bar}^{-1}\text{s}^{-1}] \\
 P_{CO} &= \text{Partial pressure of CO, [bar]} \\
 P_{H_2} &= \text{Partial pressure of H}_2, \text{ [bar]} \\
 \Delta G_{phy} &= \text{Physisorption energy of olefins, [J/mol]} \\
 n &= \text{Carbon number} \\
 \lambda_{H_2} &= \text{Charge transfer coefficient of H}_2, [-]
 \end{aligned}$$

Equation: 3.10c represents the ratio of the desorption of olefins to paraffins. Formation and desorption of paraffins is enhanced due to increase in the adsorbed hydrogen on the surface. In order to account for the change in the production of paraffins due to EPOC, partial pressure of  $H_2$ , ( $P_{H_2}$ ) is multiplied with  $\exp(-\lambda \cdot \frac{e\Delta V}{k_b T})$ . The values of  $k_o/k_p$  is 4.5005 which is calculated by fitting the equation: 3.10c to the experimental data [50], and  $\frac{\Delta G_{phy}}{RT}$  is taken as 0.2 [94].

Equations derived in sub-sections: 3.2.2, 3.2.3 and 3.2.4 are also used to study the combined effect of EPOC with temperature,  $H_2 : CO$  feed ratio and operating pressure. The results obtained from the combined studies are reported in section: 4.3 in Chapter: 4.

### 3.2.5 Continuous Stirred Plug Flow Reactor

A CSTR plug flow reactor model has been developed to study the influence of pressure along with EPOC on FT. Macro kinetic approach has been adopted. For the overall reaction rate, equation: 3.9. has been used. For each reactant and product, they are multiplied by their respective stoichiometric coefficients.

Reactant

$$\frac{\partial C_i}{\partial t} = \frac{Q}{V_{reactor}}(C_i^{in} - C_i) - \nu_i \cdot \rho_{cat} \cdot r \quad (3.11)$$

Product

$$\frac{\partial C_i}{\partial t} = \frac{Q}{V_{reactor}}(C_i^{in} - C_i) + \nu_i \cdot \rho_{cat} \cdot r \cdot m_f \quad (3.12)$$

Equation: 3.11 and equation: 3.12 are used to calculate the variations in concentration of the reactants and products respectively. To calculate the temporal variations in concentration for the products of different carbon lengths, their respective molar fractions are multiplied to the overall reaction rate.

where,

$$\begin{aligned}
 Q &= \text{Volumetric Flow Rate, [m}^3\text{/s]} \\
 V_{reactor} &= \text{Volume of the reactor, [m}^3] \\
 C_i^{in} &= \text{Inlet Concentration of the species, [mol/m}^3] \\
 \nu_i &= \text{Stoichiometric coefficient, [-]} \\
 \rho_{cat} &= \text{Catalyst density, [kg/m}^3] \\
 r &= \text{Reaction rate, [mol/m}^3\text{/s]} \\
 m_f &= \text{Molar fraction, [-]}
 \end{aligned}$$

### 3.3 Application of Periodic Potential

#### 3.3.1 Transport of Ions

For the application of periodic potential, knowing the time scale in which the ions reach the catalyst surface is vital. This will actually set a limit on the possible magnitude of the frequency for the input waveform. For this purpose, one dimensional diffusion equation is solved which is shown by equation: 3.13.

$$\frac{\partial C_i}{\partial t} = D_i \frac{\partial^2 C_i}{\partial x^2} \quad (3.13)$$

where,

$$C_i = \text{Concentration of promoter, [mol/m}^2\text{]}$$

$$D_i = \text{Diffusion coefficient of the promoter, [m}^2\text{/s]}$$

Initial and boundary conditions for equation: 3.13 are given below.

$$C_i(x, t = 0) = 0$$

$$\frac{\partial C_i(x = 0, t)}{\partial x} = \frac{J}{nF}$$

$$\frac{\partial C_i(x = L, t)}{\partial x} = 0$$

Also, using equation: 3.1b corresponding catalyst potential can be calculated. In this equation,  $\theta$  has to be calculated first, which is as follows:

$$\theta = \frac{C_i}{N_M} \quad (3.14)$$

where,

$$N_M = \text{Total moles of sites available per unit catalyst surface area}$$

$$V_{\text{catalyst}} = V_{\text{ref}} + \Delta V \quad (3.15)$$

where,

$$V_{\text{catalyst}} = \text{Catalyst potential, [V]}$$

$$V_{\text{ref}} = \text{Reference potential beyond which the surface coverage is zero, [V]}$$

$$\Delta V = \text{Change in catalyst potential wrt reference potential, [V]}$$

#### 3.3.2 Periodic Electrochemical Promotion of Catalysis for Fischer Tropsch Reaction

This subsection includes the plug flow model to study the effect of periodic application of *EPOC* on *FT* reaction. This involves the effect of frequency, symmetry of the input signal and its amplitude on the reaction. Equation for the reactant conversions is identical to equation: 3.11 discussed in subsection: 3.2.5. Equation: 3.12 for formation of product described in subsection: 3.2.5 cannot be used for the periodic application of potential. Because this equation involves the weight fraction defined by *Schulz - Flory* expression and it is valid only for steady state adsorption of *CO* and *H<sub>2</sub>* molecules [86].

$$\frac{\partial C_i}{\partial t} = \frac{Q}{V} (C_i^{\text{in}} - C_i) + v_i \cdot \rho_{\text{cat}} \cdot r_{\text{prod}} \quad (3.16a)$$

$$r_{\text{prod}_{\text{paraffins}/\text{CH}_4}} = k_{\text{paraffins}/\text{CH}_4} \cdot P_{\text{CO}}^p \cdot P_{\text{H}_2}^q \quad (3.16b)$$

$$r_{\text{prod}_{\text{olefins}}} = k_{\text{olefins}} \cdot \exp\left(-\frac{\Delta G_{\text{phy}}}{RT} \cdot n\right) \cdot P_{\text{CO}}^p \cdot P_{\text{H}_2}^q \quad (3.16c)$$

where,

$$k_i = \text{Rate constant for product } i, [\text{mol}/(\text{kg}_{\text{cat}} \text{ bar}^{p+q} \text{ s})]$$

$$v_i = \text{Stoichiometric coefficient}, [-]$$

$$G_{\text{phy}} = \text{Physisorption energy of olefins}, [\text{J}/\text{mol}]$$

$$p = \text{Exponential power of } P_{\text{CO}}, [-]$$

$$q = \text{Exponential power of } P_{\text{H}_2}, [-]$$

Equation: 3.16a is used to calculate the concentrations of the products formed during the reaction. The rate of formation of individual product is assumed to be a function of  $p^{\text{th}}$  power of  $\text{CO}$  and  $q^{\text{th}}$  power of  $\text{H}_2$  which is given by equation: 3.16c. The values of  $k_i$ ,  $p$  and  $q$  are fitted to the data provided by Williams and Lambert [50] using *fminsearch* function in *MATLAB*. It consists the values of  $\text{CH}_4$ ,  $\text{C}_2\text{H}_4$ ,  $\text{C}_2\text{H}_6$ ,  $\text{C}_3\text{H}_6$  and  $\text{C}_4\text{H}_8$ . Data for  $\text{C}_3\text{H}_8$  and  $\text{C}_4\text{H}_{10}$  are calculated using equation: 3.17. The values of these parameters are shown below in table: 3.4.

$$r_{(\text{C}_3\text{H}_8 / \text{C}_4\text{H}_{10})} = \frac{r_{(\text{C}_3\text{H}_6 / \text{C}_4\text{H}_8)}}{OP} \quad (3.17)$$

In equation: 3.17, the term  $OP$  represents olefin-paraffin ratio which is shown in equation: 3.10c.

Table 3.4: Values of the parameters  $k_i$ ,  $m$  and  $n$  used in equation: 3.16c

Product	$k_i$	$p$	$q$
$\text{CH}_4$	$1.23 \cdot 10^{-07}$	0.298	1.250
$\text{C}_2\text{H}_4$	$2.99 \cdot 10^{-09}$	-0.681	-0.199
$\text{C}_2\text{H}_6$	$4.6 \cdot 10^{-09}$	0.554	1.837
$\text{C}_3\text{H}_6$	$3.17 \cdot 10^{-09}$	-0.630	-0.151
$\text{C}_3\text{H}_8$	$5.82 \cdot 10^{-09}$	0.594	2.016
$\text{C}_4\text{H}_8$	$2.43 \cdot 10^{-09}$	-0.098	0.136
$\text{C}_4\text{H}_{10}$	$1.04 \cdot 10^{-09}$	0.248	1.45

### 3.4 Solid Oxide Fuel Cell (SOFC) type Reactor

One of the promising reactor design for *EPOC* is Solid Oxide Fuel Cell. This is because the reactor cell used in *EPOC* is almost identical to that of *SOFC* cell. Therefore, when it comes to scaling up, *SOFC* reactor might be a good option to analyse.

An *SOFC* reactor consists of the following compartments:

1. Interconnect
2. Gas Channels
3. Fuel Electrode
4. Solid Electrolyte
5. Air Electrode

Interconnect acts as the separator between two consecutive *SOFC* cells. It also contains the gas channels which carries the reactants and products along its length. As the names suggest, fuel electrode is adjacent to the gas channel through which fuel passes and air electrode is adjacent to the air channel. In the context of *EPOC*, there are working and counter electrodes. Here, working electrode is the catalyst layer and counter electrode is present on the other side of the electrolyte to complete the electrical connection. Unlike *SOFC*, the *EPOC* reactor does not always need a gas to be passed through the channels adjacent to the counter electrode.

For example,  $Na - \beta'' - aluminate$  contains  $Na^+$  ions which get transferred to the catalyst material on application of current or potential. This acts as an electrolyte. Thus, the solid electrolyte is needed for the transfer of ions to the working electrode. Reference electrodes are also used in *EPOC* to measure the absolute potential of the catalyst surface. This is possible as the reference electrode is not electrically connected to the circuit.

In the present study,  $Na - \beta'' aluminate$  is used as the solid electrolyte. It is a conductor of  $Na^+$  ions. Ruthenium is used as the catalyst or the working electrode and palladium is considered as the counter electrode. A square shaped flat plate cell has been considered whose length and breadth are  $20\text{ cm}$ . The thickness of the catalyst is assumed to be  $20 \cdot 10^{-8}\text{ m}$ . Figure: 3.1 shows the unit reactor cell with the necessary dimensions.

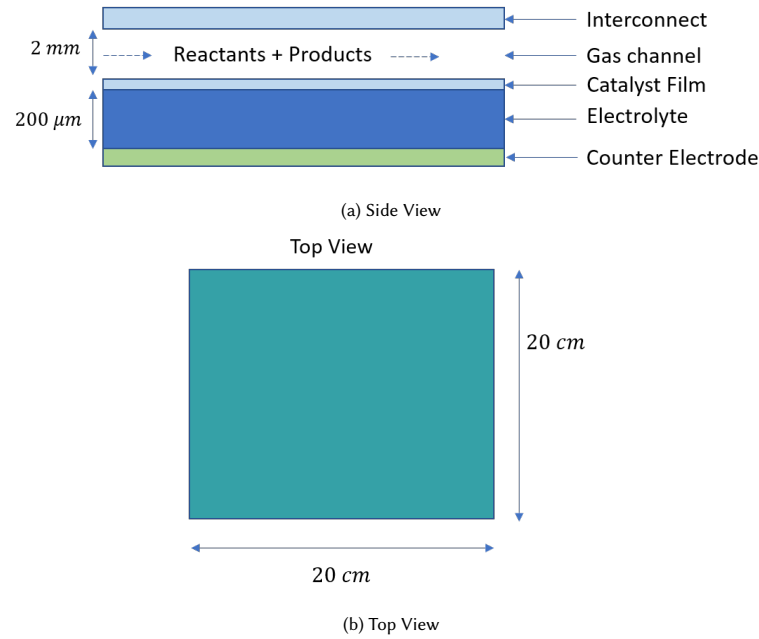


Figure 3.1: Side and Top View of *SOFC* type unit reactor cell for *EPOC*

Plug flow type reactor has been assumed for this study based on the approach adopted for steam electrolysis in Solid Oxide Electrolysis, (*SOE*) reactor by *Udagawa et al* [96]. This has been assumed here because the reactors are of similar nature. Steady state has been considered and no mass transport limitation has been taken inside the channel. Mass transport limitations had to be considered if there were liquid products formed or if any liquid was fed at the inlet of the reactor. This is the case with conventional reactors for *FT* process. But from the experiments on *EPOC* based *FT* process, it showed that negligible amount of liquid phase products are formed [51], [50]. Also only gaseous reactants are fed at the inlet, devoid of any liquid medium. Based on these assumptions, the species transport equation has been modelled which is shown by equation: 3.18.

$$u \frac{dC_i}{dx} = -v_i \cdot \rho_{cat} \cdot r \quad (3.18)$$

where,

$$u = \text{velocity, [m/s]}$$

$$C_i = \text{Concentration of the reactant } i, [\text{mol/m}^3]$$

$$v_i = \text{Stoichiometric coefficient of reactant } i, [-]$$

$$\rho_{cat} = \text{Density of the catalyst, [kg/m}^3]$$

$$r = \text{reaction rate, [mol/(kg}_{cat} \text{ s)]}$$

Effect of temperature has also been studied. There are two ways to calculate the temperature profile in the

*SOFC* reactor. One can either evaluate separate temperature profiles for all the compartments in the reactor or can have one lumped equation. These are called local temperature non equilibrium (*LTNE*) and local temperature equilibrium approach (*LTE*) respectively [97]. For simplicity, *LTE* approach is used here.

**Local Temperature Equilibrium :** This approach assumes that the temperature of all the compartments in the *SOFC* reactor are in equilibrium. An one dimensional lumped temperature profile is assumed whose variation is along the length of the reactor. This is shown in equation: 3.19.

$$\rho_{gas} c_{p_{gas}} \cdot u \frac{dT}{dx} = k_{eff} \frac{d^2T}{dx^2} + \Delta H \cdot r \quad (3.19)$$

In equation 3.19,  $k_{eff}$  is the average thermal conductivity which includes the conductivities of the interconnect, reactant gas, catalyst material, solid electrolyte and counter electrode. This is shown by equation: 3.20

$$k_{eff} = \frac{t_{int} \cdot k_{int} + t_{ch} \cdot k_{gas} + t_{cat} \cdot k_{cat} + t_{elec} \cdot k_{elec} + t_c \cdot k_c}{t_{int} + t_{gas} + t_{cat} + t_{elec} + t_c} \quad (3.20)$$

where,

$$\begin{aligned} \rho_{gas} &= \text{Density of the gas, [kg/m}^3\text{]} \\ c_{p_{gas}} &= \text{Specific heat capacity, [J/(kg K)]} \\ u &= \text{Inlet velocity, [m/s]} \\ k_{int} &= \text{Thermal conductivity of the interconnect, [W/m K]} \\ k_{gas} &= \text{Thermal conductivity of the gas, [W/m K]} \\ k_{elec} &= \text{Thermal conductivity of the electrolyte [W/m K]} \\ k_{cat} &= \text{Thermal conductivity of the catalyst [W/m K]} \\ k_c &= \text{Thermal conductivity of the counter electrode [W/m K]} \\ t_{int} &= \text{Interconnect thickness, [m]} \\ t_{elec} &= \text{Electrolyte thickness, [m]} \\ t_{cat} &= \text{Catalyst thickness, [m]} \\ t_{ch} &= \text{Gas channel thickness, [m]} \\ t_c &= \text{Counter electrode thickness, [m]} \\ T &= \text{Temperature, [K]} \\ \Delta H &= \text{Heat of reaction, [J/mol]} \end{aligned}$$

The values of the parameters used in equations: 3.19 and 3.20 are listed in table:3.5 and 3.6. Table: 3.5 consists of the thermal conductivities of the different materials present in the reactor and table: 3.6

Table 3.5: Thermal conductivities for different components of the reactor:3.20

Components	Values, [W/(m K)]
$k_{int}$	30
$k_{gas}$	0.1638
$k_{elec}$	35
$k_{cat}$	100
$k_c$	70

Table 3.6: Constants for equation:3.20

Components	Values, [m]
$t_{int}$	$200 \cdot 10^{-6}$
$t_{ch}$	$2 \cdot 10^{-3}$
$t_{elec}$	$50 \cdot 10^{-6}$
$t_{cat}$	$20 \cdot 10^{-8}$
$t_c$	$20 \cdot 10^{-6}$

Equations: 3.18 and 3.19 are solved simultaneously to calculate the variations in reactant conversion and temperature along the length of the reactor. These equations have been used to compare the results for the reactant conversion between the fitted expression and the original *Yates* and *Satterfield* [77] expression.



## Chapter 4

# Results and Discussions

This chapter deals with understanding of the effect of electrochemical promotion of catalysis on Fischer Trop-sch reaction which is done through theoretical modelling. Periodic operation of electrochemical promotion of catalysis has also been studied to investigate if any significant modification could be observed. Further, the performance of *EPOC* on a square shaped flat plate *SOFC* reactor has been evaluated. *SOFC* type reactors have been chosen because the basic cell structure of the *EPOC* reactors and *SOFC* cells are similar. Assump-tions made for the study of reactor have been discussed in section: 3.4 of Chapter: 3.

But before exploring how *EPOC* modifies the *FT* reaction, it is important to understand the effect of the applied potential on the promoter coverage. This coverage of the ions will modify the reaction.

### 4.1 Surface Coverage of Promoter Ion

As shown in equation: 3.1 in Chapter: 3, there is a linear relationship between the promoter coverage and the applied potential. The equation also shows that dipole moment of the ion has a role to play on the coverage. The value of which changes according to the type of ion. Depending on the dipole moment, one can have different coverage at the same applied potential.

In this case, sodium has been used as the promoter ion. Figure: 4.1 shows the potential dependent coverage of ions.  $0.4V$  has been chosen as the reference potential as this is the lowest potential at which the catalyst surface is devoid of any promoter ion. This was found experimentally by *Williams* and *Lambert* [50] for *Na* promotion for *FT* reaction on Ruthenium (*Ru*) catalyst.

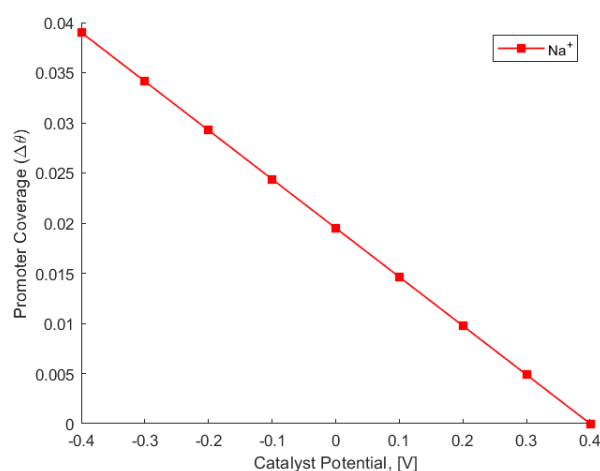


Figure 4.1: Change in surface coverage of promoter ion ( $Na^+$ ) with the catalyst potential.

From the fig: 4.1, it can be concluded that as the potential is decreased, the promoter coverage increases. This is because  $Na^+$  is a cation and would get transported towards more negative or lower potential. Conversely, anions like  $P^{3-}$  or  $B^{3-}$  would have transported from negative to positive potential. The magnitudes of promoter coverage shown in fig: 4.1 is in range with that experimentally determined by *Williams et al* [98]. At  $-0.6 V$ , they found 6% coverage of  $Na$  ions on *Copper* surface.

## 4.2 Electrochemical Promotion of Catalysis on Fischer Tropsch Reaction

### 4.2.1 Chain Growth Probability

In this work, the effect of alkali promotion on the chain growth probability has been studied. Figure: 4.2a shows the variation of the chain growth probability with the catalyst potential. It shows that on decreasing the potential or equivalently increasing the alkali coverage, the chain growth probability increases. Thus, from the figure, it can be concluded that the probability of producing longer carbon chains increases with increasing in alkali loading. The equation: 3.6 is fitted to the experimental data provided by *Williams and Lambert* [50]. Similarly, figure: 4.2b shows the variation of chain growth probability with the catalyst potential for the expression provided by *Vervloet et al* [93]. The expression is fitted to the same set of experimental data [50].

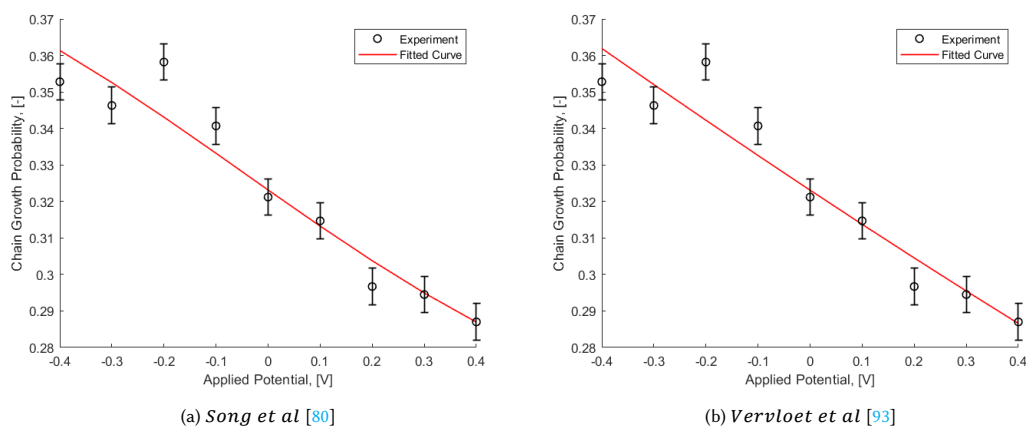


Figure 4.2: Variation of chain growth probability with different catalyst potentials using equations by *Song et al* and *Vervloet et al*

Both figures: 4.2a and 4.2b shows similar trends after modifying the expressions to account for the effect of the catalyst potential. The figures depict an increasing trend of chain growth probability with decreasing catalyst potential or increasing coverage of alkali atoms.

One possible reason for the enhancement in chain growth probability could be due to improved adsorption and dissociation of  $CO$  molecules on the catalyst surface. At the same time adsorption of  $H_2$  is decreased with the alkali loading. These changes can be attributed to the electronic nature of the molecules. Here,  $CO$  acts as an electron acceptor and  $H_2$  acts an electron donor. The alkali atoms on the catalyst surface form dipoles. They acquire positive charge and the metal catalyst surface acquires negative polarisations. Such an electron rich surface makes the adsorption for electron acceptors (like  $CO$ ) favourable. Increase in the adsorption of  $CO$  indicates more number of carbon atoms available for chain growth. Thus, alkali promotion is favourable in increasing the chain growth probability of the  $FT$  reaction.

### 4.2.2 Reaction Rate

Even though, the alkalis are coined the term promoters for the  $FT$  reaction, they actually lower the reaction rate. Figure: 4.3 clearly shows decreasing trend in the overall rate of reaction with lowering the potential or increasing the alkali loading on the catalyst surface.

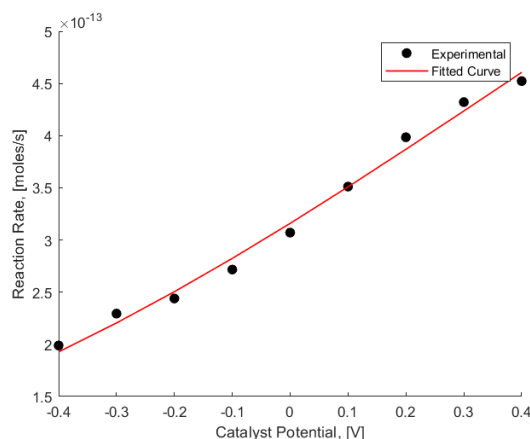


Figure 4.3: Effect of changing catalyst potential on the overall reaction rate.

Reaction rate is calculated using the expression given by *Yates and Satterfield* [77]. The values of the factors  $a$  and  $b$  in the equation: 3.9 have been calculated by fitting the expression to the experimental data provided by *Williams and Lambert* [50]. The reason for doing so is to match the lower activity per unit mass of the catalyst film compared to those used in original Fischer Tropsch reaction. For identical conditions, the magnitude of the original reaction rate is higher than that of the modified version. One reason for lower activity is due to the dense structure of the catalyst film. The catalyst film is needed to be dense, so that the entire catalyst retains the electrical conductivity. But in the process it loses a lot of active surface area and consequently, activity of the catalyst face adverse effects.

From the equation: 3.9, it is clear that concentration of  $H_2$  acts as a more dominant factor than that of  $CO$ . Thus, decreasing hydrogen adsorption due to alkali coverage reduces the magnitude of the reaction rate. This also suggests that the *FT* reaction is electrophobic in nature which means its magnitude increases with increase in the applied potential [22]. Moreover, from the rules of promotion stated by *Vayenas et al* [22], it is clear that for an electrophobic reaction, the adsorption of electron donor molecules are much lower than that of the electron acceptor molecules. Therefore, with increase in alkali loading or reducing catalyst potential,  $H_2$  adsorption becomes more rate limiting.

### 4.2.3 Olefin-Paraffin Ratio

*Olefin – Paraffin* ratio increases with alkali loading as shown in fig: 4.4. Equation: 3.10c has been fitted to the experimental data [50] for the ratio between  $C_2H_4$  and  $C_2H_6$ .

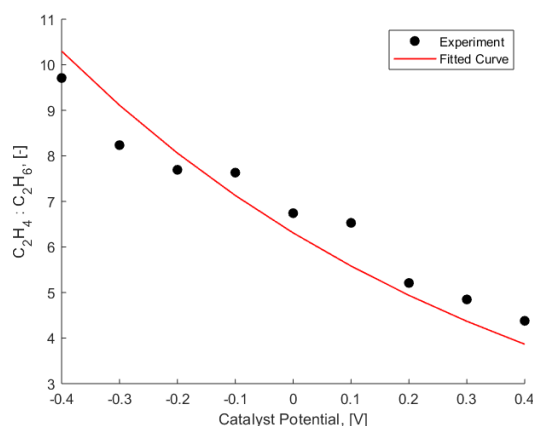
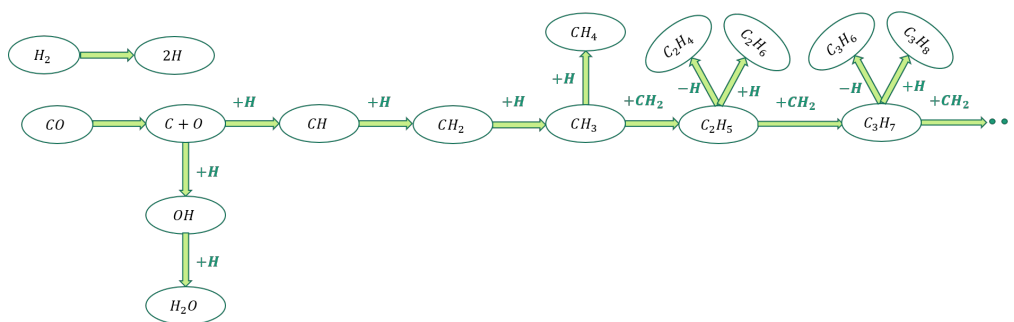


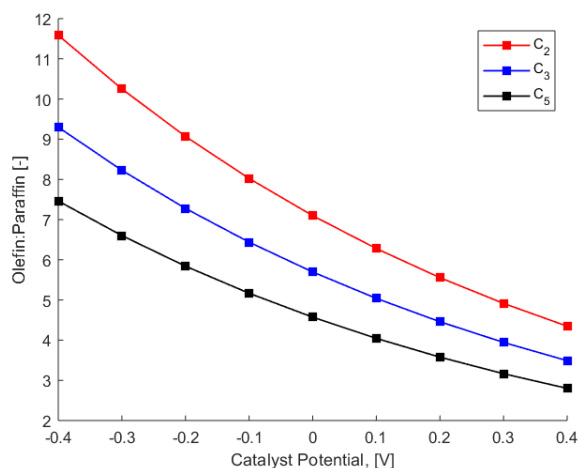
Figure 4.4: Variation of *olefin – paraffin* ratio for  $C_2$  wrt catalyst potential.

Figure 4.5: Carbide Mechanism for *FT* reaction.

This can be explained using the carbide mechanism for *FT* as shown in fig: 4.5, where olefins and *n*-paraffins are the products. Olefins are formed by the elimination of the  $\beta$ -hydrogen atom and *n*-paraffins are produced by adding adsorbed hydrogen to the  $\alpha$  position of the carbon chain. Since, hydrogen adsorption is reduced due to alkali loading, therefore, formation of *n*-paraffins is decreased. As a result olefin to paraffin ratio increases.

However, it is not very certain that olefin production increases with alkali loading. This is because contradicting results are displayed for olefin production in literature. *Williams* and *Lambert* showed that even though selectivity of olefin formation increases, but in reality, the rate of olefin production decreases with increasing sodium promoter over *Ruthenium* catalyst [50]. Increase in selectivity is backed by the fact that the decrements in olefin production are lower than that of paraffin production [50]. *Urquhart et al* reported an increase in olefin production with decrease in potential or increase in potassium coverage over *Rhodium* catalyst [51]. But drop in paraffin production with increasing alkali loading was common to both the works.

Figure: 4.6 shows the *olefin – paraffin* ratio for different carbon lengths for  $H_2 : CO$  ratio equal to 2. It shows that as the length of the carbon chain increases, the magnitude of the *olefin – paraffin* ratio decreases. This is because the ratio is inversely proportional to the exponential of carbon number as shown in equation: 3.10c. This has been backed by experimental evidence reported by *Kuipers et al* [94] and *Iglesia et al* [81]. Moreover, for each carbon number, the ratio decreases with increasing catalyst potential.

Figure 4.6: Variation of *olefin – paraffin* ratio for  $C_2$ ,  $C_3$  and  $C_5$  wrt catalyst potential.

### 4.3 Combined Effect of Operating Conditions and *EPOC* on *FT*

This section deals with the study of the combined effects of *EPOC* and operating conditions on *FT*. Mainly, role of temperature,  $H_2 : CO$  feed ratio and pressure are investigated. The purpose of this section is to see how the variations in these operating parameters influence the *FT* along with the effect of alkali loading. This kind of study can help in choosing the right operating conditions for the process.

### 4.3.1 Temperature + EPOC

Effects of temperature on chain growth probability and reaction rate have been studied in this section. Figures: 4.7a and 4.7b show the combined effect of variations in temperature and applied catalyst potential on the chain growth probability and the reaction rate respectively. The surface plot for chain growth probability suggests that lower temperature and more negative catalyst potential are favourable for the selectivity towards longer hydrocarbon chains. Whereas, the surface plot for the reaction rate shows its maximum magnitude towards higher temperature and more positive potential. The variations in chain growth probability and reaction rate with temperature are more pronounced than those with the applied catalyst potential or sodium coverage.

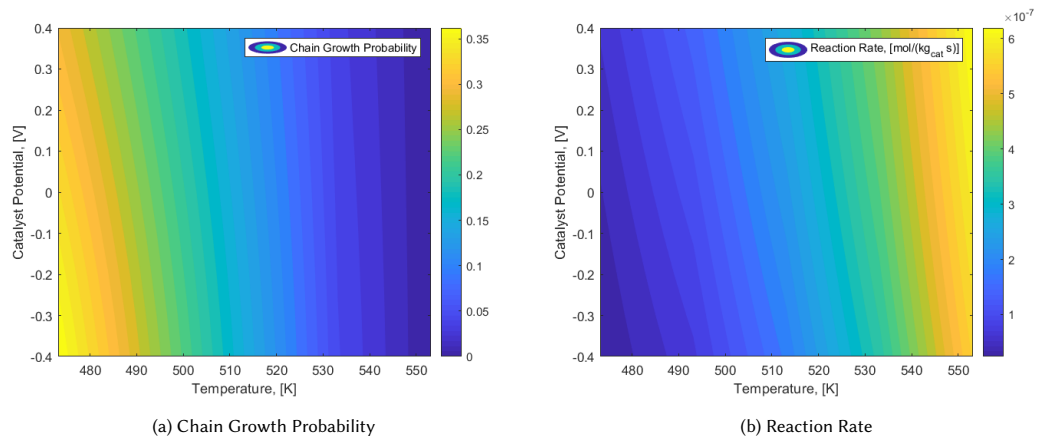


Figure 4.7: Variation of chain growth probability and reaction rate with different temperatures and catalyst potentials.

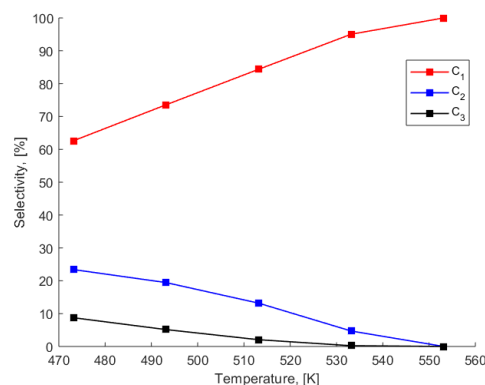


Figure 4.8: Variation in Selectivity of  $C_1$ ,  $C_2$  and  $C_3$  as a function of temperature at an applied catalyst potential of  $-0.4V$ .

Even though, the reaction rate is very high towards higher temperature, but chain growth probability tends to zero in this zone. This means, methane will be the sole product formed at higher temperature. This is shown in fig: 4.8 where 100% selectivity for methane is observed at 553.15 K. If longer hydrocarbon chains are desired then one has to compromise with the reaction rate, provided all other operating conditions are fixed.

### 4.3.2 $H_2 : CO$ Ratio + EPOC

The influence of  $H_2 : CO$  ratio on reaction rate and chain growth probability has been studied in this section. Figures: 4.9a and 4.9b show the combined effect of  $H_2 : CO$  ratio and applied catalyst potential on reaction rate and chain growth probability respectively. From fig: 4.9a, it can be inferred that with increasing  $H_2 : CO$  ratio, the reaction rate first increases, reaches a maximum value and then starts decreasing. Whereas, with decreasing the catalyst potential, the reaction rate decreases. This suggests that the decrease in reaction rate due to the EPOC effect can be compensated with increase in  $H_2 : CO$  ratio.

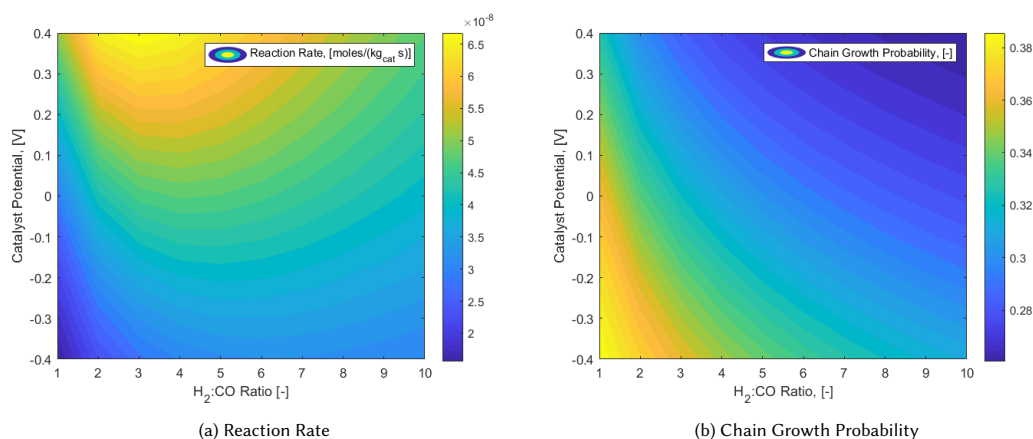


Figure 4.9: Variation of reaction rate and chain growth probability with  $H_2 : CO$  ratio at different catalyst potentials.

Chain growth probability decreases with increase in the  $H_2 : CO$  ratio. Whereas, it increases with lowering the catalyst potential or equivalently increasing the sodium coverage over the catalyst. If longer hydrocarbons are desired, then the  $H_2 : CO$  ratio should not be high. Otherwise, it will oppose the enhancement in the chain growth probability caused by *EPOC* on the reaction.

### 4.3.3 Pressure + *EPOC*

Influence of operating pressure can be felt on the reaction rate and the residence time of the reactor. Figure: 4.10a shows an increase in reaction rate with increasing pressure. In lower pressure regime (*till*  $\sim 4$  bar), a faster growth in the reaction rate can be observed. Further with increasing pressure, the growth slows down.

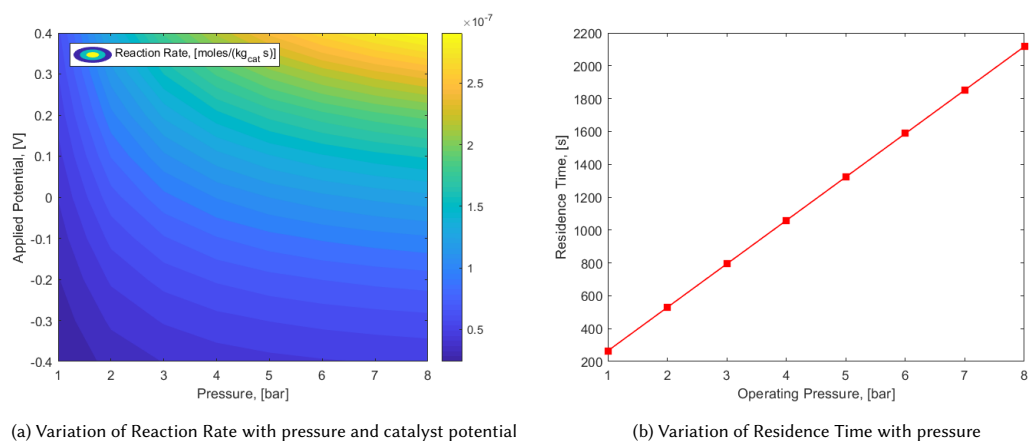


Figure 4.10: Variation of reaction rate and residence time as a function of pressure.

Effect of pressure on residence time has been studied using a plug flow reactor configuration. The study is carried out by varying pressure in the range 1–8 bar.  $H_2 : CO$  ratio is kept at 2 : 1 and isothermal operation is assumed. The reactor volume is  $70 \text{ cm}^3$  and a flow rate of  $10 \text{ mL/min}$  is taken. Fig: 4.10b shows an increase in residence time towards higher pressure. This means that the reactants get more time to participate in the reaction. Therefore, both the improvement in reaction rate and the residence time will improve the conversion of the reactants. Thus, higher pressure operation can compensate the decrease in the reaction rate due to the *EPOC* effect.

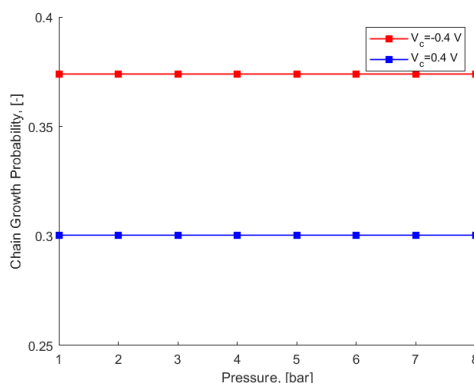


Figure 4.11: Effect of pressure on chain growth probability at different catalyst potential.

Unlike the effect of temperature and  $H_2 : CO$  ratio, operating pressure does not decrease the chain growth probability as can be seen in fig: 4.11. Rather, pressure does not have any effect on the magnitude of the chain growth probability.

## 4.4 Dynamic Electrochemical Promotion of Catalysis

This section deals with the periodic application of potential on the  $FT$  reaction. Periodicity is applied to the reaction in the form of a square wave. The study of the periodicity can be done using three parameters related to the wave form. They are frequency, symmetry or duty cycle of the period and the amplitude of the wave.

### 4.4.1 Effect of Frequency

The effect of frequency will depend on two time scales. One is the diffusion time scale. It is the time taken by the promoter ions to reach the catalyst surface via diffusion. The second time scale is associated with the kinetics of the reaction. Both of these time scales have to be taken care of while imposing any kind of periodicity to the process. Diffusion of ions through metal catalyst film is very slow. Diffusion coefficient can be in the order of  $\sim 10^{-15}$ ,  $[m^2/s]$  [99] or even lower. Slow diffusive transport can pose significant limitation to the application of periodicity with higher frequency.

Transport equation (3.13) described in section: 3.3.1 in Chapter: 3 is solved to understand the effect of frequency on the coverage of the ions on the catalyst surface. A square wave with maximum and minimum current values of  $120, \mu A$  and  $20, \mu A$  respectively is used as an input which will be responsible for the generation of the promoter ions at the electrode electrolyte interface. The necessary parameters assumed in the calculation are shown in table: 4.1.

Table 4.1: Constants for equation:3.9

Constants	Values
Film thickness ( $t_c$ )	1, 0.1 [ $\mu m$ ]
Waveform	Square
$I_{min}$	20 [ $\mu A$ ]
$I_{max}$	120 [ $\mu A$ ]

Figures: 4.12 and 4.13 show the variation of surface coverage of the promoter species as a function of time due to the periodic application of current at different frequencies. Results for two catalyst film thickness ( $t_c$ ) has been given. They are  $0.1 \mu m$  and  $1 \mu m$  thick depicted in figs: 4.12 and 4.13 respectively. With increasing film thickness, the effect of the frequency of the fluctuations on the promoter coverage become less visible. This is because of the limitations posed by the slow diffusive transport. At  $1 Hz$ , the promoter coverage for the  $1 \mu m$  thick film show steady state kind of behaviour which is shown in fig: 4.13b. Whereas, for  $0.1 \mu m$  thickness,

still some fluctuations can be observed for the case of 1 Hz frequency. This can be seen in fig: 4.12b. If higher frequency is needed to be incorporated to the process, then the catalyst film thickness should be made smaller to avoid diffusion limitations of the promoter ions.

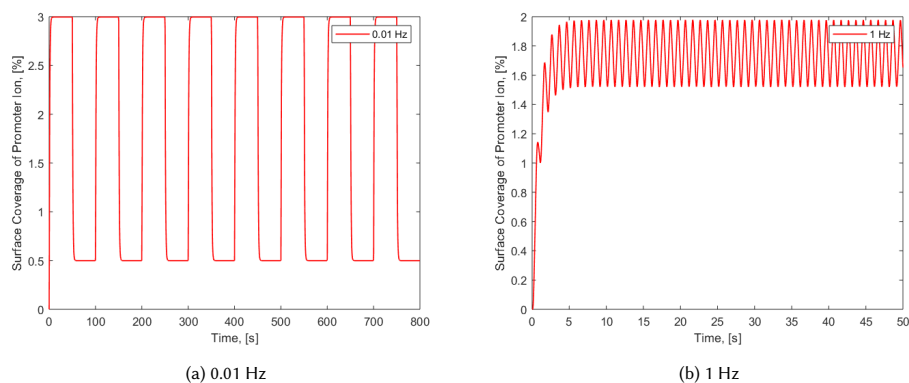


Figure 4.12: Variation of promoter coverage on the surface of a catalyst film of thickness 0.1  $\mu m$  at frequencies of 0.01 Hz and 0.01 Hz.

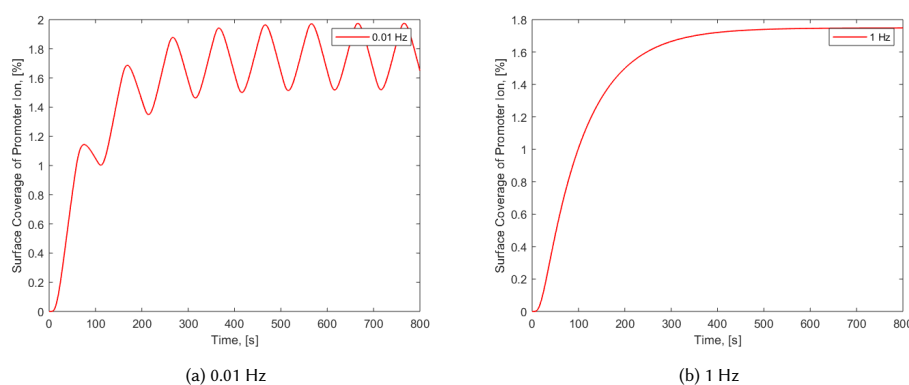


Figure 4.13: Variation of promoter coverage on the surface of a catalyst film of thickness 1  $\mu m$  at frequencies of 0.01 Hz and 0.01 Hz.

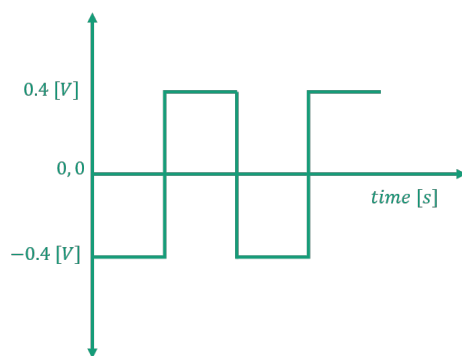


Figure 4.14: Input signal of catalyst potential

Further, the effect of frequency has been studied for the *FT* reaction. For that, a symmetric square wave formed by  $-0.4 V$  and  $0.4 V$  is chosen as the input signal which is shown in fig: 4.14.

Figure: 4.15 represents the effect of frequency on *CO* conversion for *FT* process. For simplicity, the diffusive transport limitation of the ions have not been considered. Such an assumption is made in order to understand the sole effect of frequency on the kinetics of the reaction. The graph is based on the modified reaction rate to

account for the low activity per unit mass of the catalyst. Although, the conversion values are negligibly small but still slight variations can be seen with changing frequency. It first increases with increasing frequency and then starts decreasing after reaching a maximum. In the lower frequency range the increment in conversion is hardly considerable, therefore, it cannot be observed clearly from the graph.

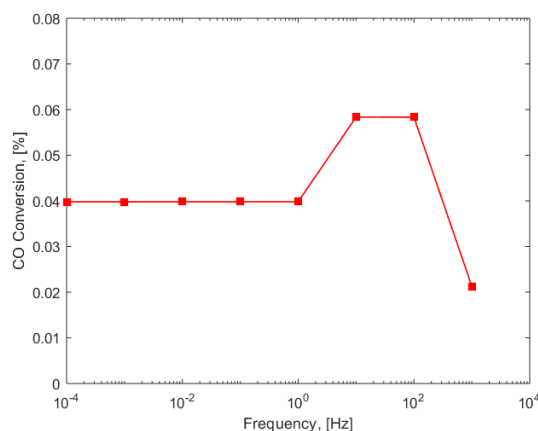


Figure 4.15: Effect of frequency on  $CO$  conversion

The trend observed in fig: 4.15 can be explained in terms of the adsorption of  $H_2$  on the catalyst surface. If the  $FT$  reaction is assumed to be electrophobic, the adsorption of the donor molecules ( $H_2$ ) should be rate limiting. *Williams* and *Lambert* found through experiments that increasing the potential, increases the  $FT$  reaction rate [50]. This indeed fits to the definition of electrophobic reactions [22]. The trend for the  $CO$  conversion is quite similar to the catalytic resonance phenomenon explained by *Ardagh et al* [38]. It states that if the frequency of surface energy oscillations is in the vicinity of the natural frequency of the reaction, then the turn over frequency is maximum in that frequency. Further increase in frequency tends to decrease the turnover frequency. Similarly, in this case,  $CO$  conversion increases until the frequency of the waveform resonates with perhaps the natural frequency of adsorption of  $H_2$ . In this range the conversion is maximum and beyond that, frequency of oscillations is too high for the adsorption of  $H_2$ . Therefore, there is a decline in  $CO$  conversion.

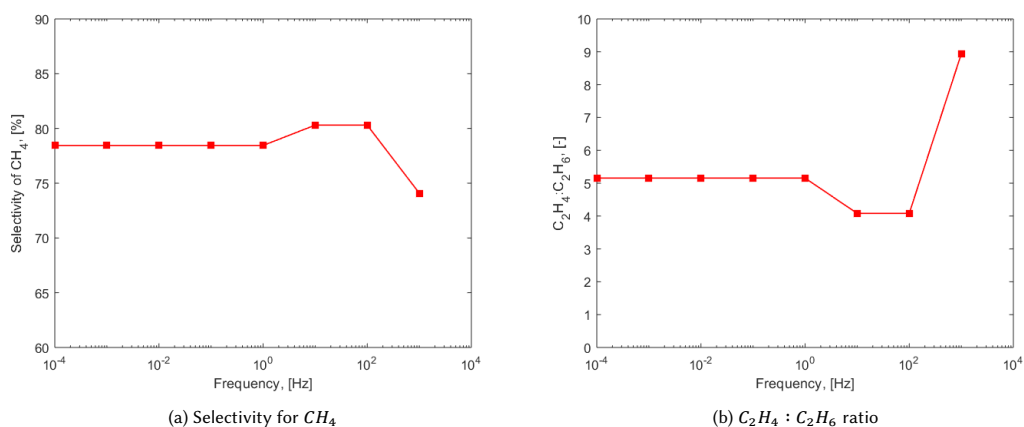


Figure 4.16: Variation of  $CH_4$  selectivity and  $C_2H_4 : C_2H_6$  ratio with increasing frequency of oscillations of the catalyst potential waveform.

Figure: 4.16a shows the variation of the selectivity of  $CH_4$  with the frequency of oscillations. It follows the similar trend as shown by  $CO$  conversion in fig: 4.15. This is because,  $CH_4$  formation is highly dependent on hydrogenation. Its maximum lies where hydrogen adsorption is maximum. The  $C_2H_4 : C_2H_6$  ratio decreases with increasing frequency, reaches a minimum for a range of frequency and beyond that the magnitude rises. The minimum is exactly in the range  $10^1$  to  $10^2$  Hz. On the  $C_2H_4 : C_2H_6$  ratio is minimum in the region where the  $CO$  conversion is maximum or in other words,  $H_2$  adsorption is at its highest magnitude. In this

region, hydrogenation of carbon chains will lead to higher growth in paraffin formation. This will lower the selectivity towards olefin and as a result olefin-paraffin ratio decreases with frequency.

Even though in the above studies, frequency up to 1000 Hz has been considered, in reality, the corresponding observations shown above may not be visible. First of all, diffusion limitations of the ions will oppose the influence of higher frequency. In such a case, the reaction will rather be influenced by the average potential of the wave form. Secondly, due to the extremely low activity per unit mass of the catalyst one may not see any changes which are of any practical value.

#### 4.4.2 Effect of Duty Cycle

Duty cycle or symmetry is an indication of the fraction of the time period for which a pulse exists. For studying the effect of duty cycle, the square waveform for the catalyst potential shown in fig: 4.14 is used here with a frequency of 0.001 Hz. An asymmetry is created by changing the fraction of  $-0.4\text{ V}$  from 10% to 90% in each cycle or period of the waveform. Effect of duty cycle on the reactant conversion, olefin – paraffin ratio, chain growth probability and selectivity of  $\text{CH}_4$  are discussed in this subsection.

Figure: 4.17a shows the variation of reactant conversion with duty cycle. Reactant conversion decreases as the fraction of more negative potential or alkali loading increases. This is because, in the process of increasing the duty cycle,  $\text{H}_2$  adsorption on the catalyst surface is reduced. This affects the reaction rate as shown in subsection: 4.2.2. Figure: 4.17b represents the variations in olefin – paraffin ratio with the increasing duty cycle. The olefin – paraffin ratio increases with the increment in the duty cycle. This is because of the presence of the more negative potential for a larger fraction of the cycle. As a result,  $\text{H}_2$  adsorption decreases and consequently rate of formation of paraffins decreases which are formed by hydrogenation. Thus, improving the selectivity towards olefins.

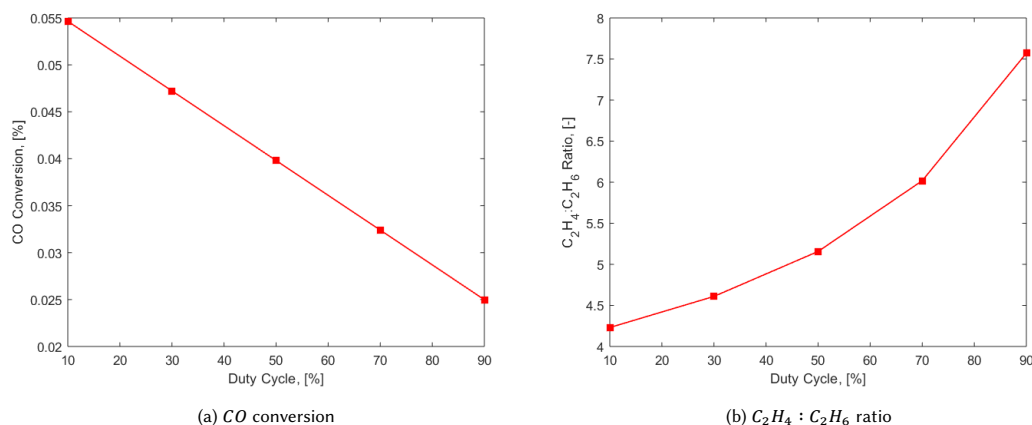
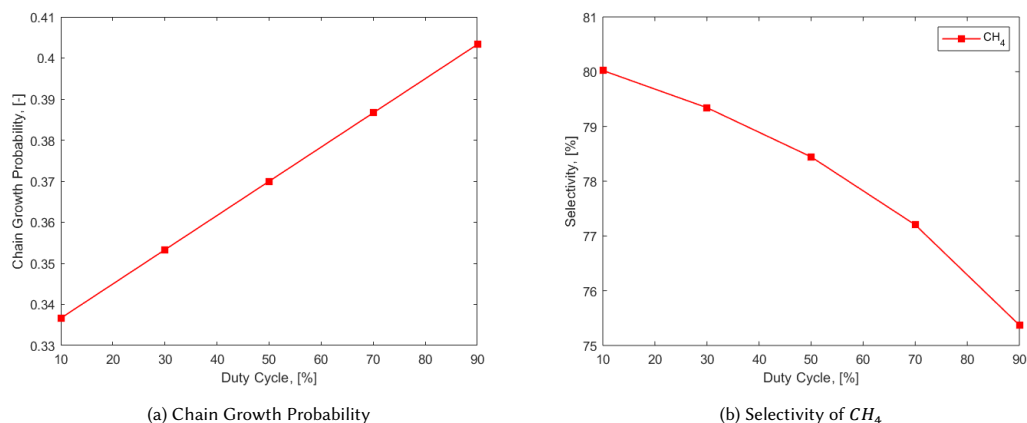


Figure 4.17: Variation of CO conversion and  $\text{C}_2\text{H}_4 : \text{C}_2\text{H}_6$  ratio with increasing duty cycle.

Figure: 4.18 shows the variation of chain growth probability and selectivity of  $\text{CH}_4$  with the duty cycle. Chain growth probability increases with increase in the duty cycle as represented by fig: 4.18a. This because with increasing duty cycle, more negative potential or higher alkali loading prevails for a longer fraction of the time period. As a result CO adsorption is increased and leads to greater probability for formation of longer carbon chains. On the other hand selectivity of  $\text{CH}_4$  decreases with increasing duty cycle as shown in fig: 4.18b. This is because with increasing the duty cycle,  $\text{H}_2$  adsorption decreases and it hampers the production of  $\text{CH}_4$ . Also, increase in the chain growth probability with duty cycle reduces the fraction of  $\text{CH}_4$  from the product distribution.

Figure 4.18: Variation of chain growth probability and selectivity of  $CH_4$  as a function of duty cycle.

Next, for the purpose of comparison between *DEPOC* and *EPOC*, the potential waveform shown in fig: 4.14 with 50% duty cycle and a frequency of 0.001 Hz is chosen. The comparison is made with its corresponding average potential value, i.e., 0 V. or the change in potential ( $\Delta V = -0.4$  V). The comparison is made based on *CO* conversion,  $C_2H_4 : C_2H_6$  ratio and  $CH_4$  selectivity.

Table 4.2: Comparison between *DEPOC* and *EPOC*.

Parameters	DEPOC	EPOC
<i>CO</i> Conversion, [%]	0.03981	0.03739
$C_2H_4 : C_2H_6$ , [-]	5.157	6.038
$CH_4$ Selectivity, [%]	78.44	77.581

The values are shown in table: 4.2. It can be observed that the magnitudes of *CO* conversion and  $CH_4$  selectivity are higher in the case of *DEPOC* whereas  $C_2H_4 : C_2H_6$  ratio is higher in case of *EPOC*. This is because with the introduction of periodicity in case of *DEPOC*,  $H_2$  adsorption increases. As a result of *CO* conversion increases and also the selectivity towards  $CH_4$  and other paraffins.

#### 4.4.3 Effect of Amplitude

The influence of the amplitudes was investigated by changing the amplitude of a symmetrical potential square wave fluctuating about 0 V. Amplitudes with magnitudes, 0.4, 0.3, 0.2 and 0.1 V are considered. The values of the maximum and minimum catalyst potentials corresponding to each amplitudes are shown in table: 4.3.

Table 4.3: Maximum and minimum catalyst potentials corresponding to different amplitudes for a symmetrical square wave.

Amplitude [Volt]	$V_{max}$ [Volt]	$V_{min}$ [Volt]
0.1	0.1	-0.1
0.2	0.2	-0.2
0.3	0.3	-0.3
0.4	0.4	-0.4

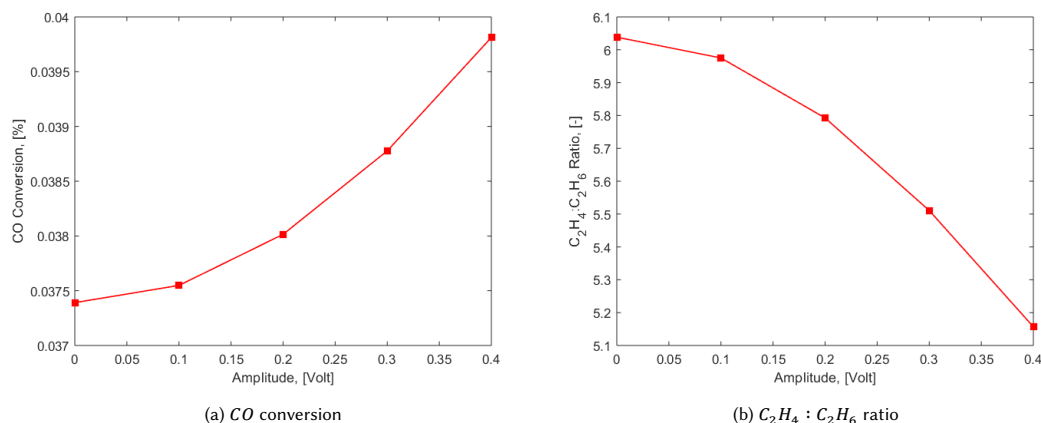


Figure 4.19: Variation of  $CO$  conversion and  $C_2H_4 : C_2H_6$  ratio as functions of the amplitude of the input potential square wave.

Figure: 4.19a shows the effect of increasing amplitude on  $CO$  conversion. From the figure, it is evident that increasing the amplitude of the input wave leads to an increase in the  $CO$  conversion. This can be explained through the fact that Fischer Tropsch exhibits electrophobic nature. Being an electrophobic reaction, adsorption of the donor molecules should be rate limiting which is  $H_2$  molecule for this case [22]. The adsorption strength of  $H_2$  is proportional to  $exp(\lambda_{H_2} \cdot \frac{e\Delta V}{k_b T})$ , i.e., it exponentially depends on the change in catalyst potential, ( $\Delta V$ ). Therefore, when the potential is periodically varied between a maximum and minimum value, on an average, the effect of adsorption will be more inclined towards the maximum value of the potential. Therefore, as the magnitude of the amplitude or equivalently maximum potential increases, hydrogen adsorption increases. The change is not very high because of the low value of the charge transfer coefficient ( $\lambda_{H_2}$ ) which is multiplied to the catalyst potential as shown above. As a result of this small improvement in  $H_2$  adsorption,  $CO$  conversion increases. This is because the reaction rate for  $FT$  depends on the adsorption of  $H_2$  molecules.

Because of the improvement in  $H_2$  adsorption, the hydrogenation of the carbon chains increases too. This results in the growth of paraffin formations. Consequently, selectivity towards olefins decreases. Thus, the olefin paraffin ratio also decreases. This has been shown in fig: 4.19b. It shows a decreasing trend in the ratio of  $C_2H_4$  and  $C_2H_6$  with the increase in the amplitude.

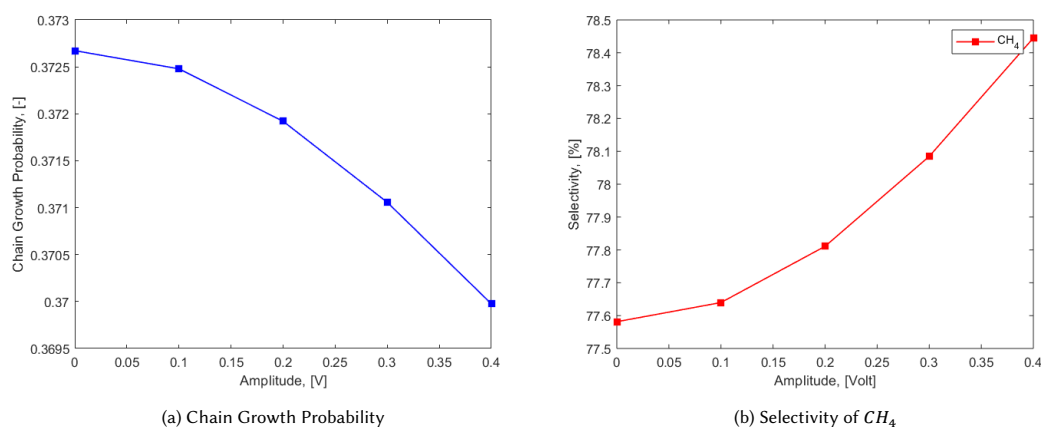


Figure 4.20: Variation of chain growth probability and selectivity of  $CH_4$  as functions of the amplitude of the input potential square wave.

Figure: 4.20a shows the variation of chain growth probability as a function of amplitude. Chain growth probability decreases with increase in the amplitude. This is again because of the improvement in the hydrogen adsorption which will lead to increase in the termination of carbon chains via paraffin formation. Further, there is obvious improvement in the selectivity of methane formation as it is highly dependent on hydrogenation. This is shown in fig: 4.20b.

In all of these cases, the variations observed are not very high. This has to do with the charge transfer coefficient of hydrogen ( $\lambda_{H_2} = 0.05$ ). If a higher value was assumed, the variations could have been more significant.

## 4.5 Reactor Design Philosophy

Reactors generally used for the study of *EPOC* are well mixed reactors. But other reactors like monolith have also been used to study the phenomenon. Monolithic reactors have been used in the study of the effect of *EPOC* on *NO* reduction [100]. Apart from this, *SOFC* type reactors are also explored for understanding the phenomenon [101]. These reactors come with their own advantages and disadvantages. For example, considering *SOFC* as a possible reactor means, all the inherent issues with such reactors will add up to the limitations of the *EPOC* effect. Issues like temperature variation, cell degradation, have to be taken into account while designing an *SOFC* type reactor [102].

### 4.5.1 Catalyst for *EPOC*

One of the issues that have hindered commercial application of *EPOC* is the use of a highly dense catalyst film to maintain electrical connectivity within the material. For a desired amount of production under same operating conditions, a larger amount of catalyst material will be required compared to any classical system. This makes the material cost highly expensive. Therefore, search for cheaper catalyst material and much thinner catalyst films are desired. Nano structured films formed by metal sputtering techniques provide the advantage of small thickness and at the same time higher dispersion ( $> 10-20\%$ ) [100]. They are comparable to the commercially available catalysts [103].

### 4.5.2 Wireless Configuration

Another issue in reactor design for *EPOC* is the involvement of wired connections. An efficient current collection system is necessary to minimise the number of wires used in the reactor [103]. This is because the competition of *EPOC* is with classical reactors rather than the electrochemical ones [103]. In order to overcome this, bipolar configurations are developed where the catalyst material is not electrically connected.  $C_2H_4$  oxidation is being studied in such a configuration [104]. In bipolar configuration there are electrode materials on either sides of the catalyst to complete the electrical connectivity [104]. The rate enhancement will be lower compared to a normally used reactor as the two halves of the catalyst are oppositely polarised due to the presence of the two electrodes adjacent to it. Another wireless configuration studied is using mixed ionic electronic conducting supports [105]. These structures can conduct both ions and electrons. Therefore, it eliminates the requirement of any wired connections [105]. Here, a sweep gas (e.g.,  $O^{2-}$ ) is used. Because of chemical potential difference, oxygen ions are transferred to the catalyst through the electrolyte membrane. These ions will act as promoters over the catalyst.

The next two subsections are about the possible issues which affects the scaling up of the electrochemically promoted Fischer Tropsch process.

### 4.5.3 Reactant Conversion for Fischer Tropsch reaction

For the study of the reactant conversion, an *SOFC* type cell has been considered. A flow rate of  $400 \text{ mL/min}$  is used in a cell of  $0.2 \text{ m} \times 0.2 \text{ m}$  dimension with channel height of  $2 \text{ mm}$ . Figure: 4.21 shows the consumption of the reactants along the length of the reactor.

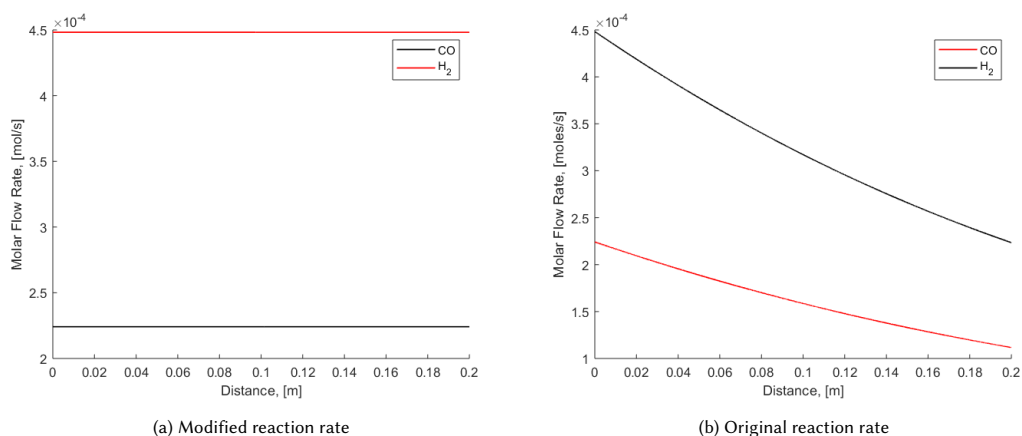


Figure 4.21: Consumption of reactants along the length of the reactor using modified reaction rate to account for the low catalytic activity in the case of *EPOC* and the original *Yates* and *Satterfield* expression.

In fig: 4.21a, modified reaction rate for *EPOC* is used and in fig: 4.21b, original *Yates* and *Satterfield* expression is used. From experimental evidence, it is clear that the original expression cannot be used in the study of *EPOC* [50]. The reason for this has been mentioned several times which is the lower activity per unit mass of the catalyst. Clearly, higher conversion is achieved in the second case. Conversion for the case with low catalytic activity is only 0.0212%, whereas in the second case, it is 50.15%. Hence, due to extremely low conversion, scaling up of the process at this stage does not seem to be feasible.

#### 4.5.4 Importance of Heat Management in Fischer Tropsch

If the activity per unit mass of the catalyst can be improved, then one needs to think about isothermal operation. This is extremely necessary for the *FT* reaction as it is highly exothermic in nature. It releases about  $170 \text{ kJ/mol}$  of heat at around  $200 \text{ }^\circ\text{C}$  [71]. As a result, the temperature along the length of the reactor can increase significantly. This will have an impact on the selectivity of the reaction. As an illustration, variation of temperature and consequent changes in the chain growth probability are calculated along the length of the reactor. For this purpose, the original *Yates* and *Satterfield* expression [77] has been used. If the modified expression for reaction rate is used then due to its low conversion temperature will not rise significantly.

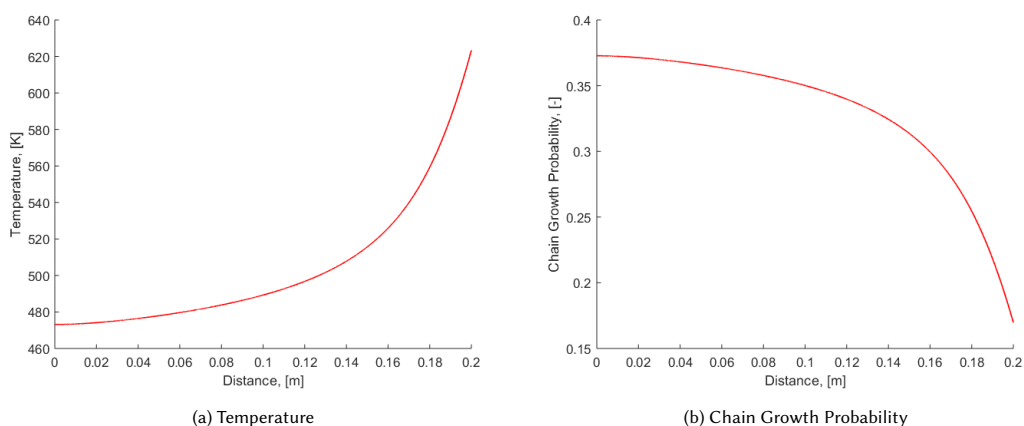


Figure 4.22: Consumption of reactants along the length of the reactor using catalyst common to *EPOC* and that used in conventional *FT* reactors.

Figure: 4.22a shows that there can be significant increase in temperature along the length of the reactor. As a result the chain growth probability also changes which perturbs the original nature of selectivity of the reaction. The decrease in chain growth probability along the length of the reactor has been depicted in fig:

4.22b. This will eventually lead to the generation of higher amount of methane. Therefore, controlling the temperature will be highly necessary to utilise the full potential of *EPOC* effect on *FT* reaction.



## Chapter 5

# Conclusion and Future Outlook

This study focused on the understanding of the effect of electrochemical promotion of catalysis on Fischer Tropsch reaction. It involves the studying the modifications that take place in the reaction due to the application of sodium as a promoter over Ruthenium catalyst. The work was carried using a theoretical approach which involved deriving analytical or semi empirical expressions to account for the phenomenon. Further, plug flow reactors were used to study the effect of dynamic electrochemical promotion of catalysis on Fischer Tropsch. Dynamic study was performed by periodic application of input potential or current to the reactor. Also, possibility of reactor designs were investigated.

### 5.1 EPOC in Fischer Tropsch

Effect of *EPOC* on *FT* was studied based on three important parameters of the reaction, i.e., chain growth probability, reaction rate and olefin-paraffin ratio. Chain growth probability increases with alkali promotion. This implies selectivity towards higher Carbon number increases with alkali promotion. Even though throughout this work and in literature [50], [51], the process has been termed as alkali promotion but in reality, reaction rate decreases with increasing alkali concentration on the catalyst surface. In other words with increase in negative potential ( $V_{WR}$ ), reaction rate decreases. Thus, Fischer Tropsch shows electrophobic behaviour. This conclusion is based on the rules provided by *Vayenas et al* [22]. Improvement in *olefin-paraffin* ratio has been observed with alkali promotion. This could be because of low hydrogen adsorption due to the presence of the sodium ions on the surface of the catalyst. Reduced adsorption of hydrogen affects the production of *n*-paraffins as they require addition of adsorbed hydrogen to their  $\alpha$  carbon atom.

Next, the influence of *EPOC* along with the operating parameters was studied. This was done in order to understand whether changes on the operating conditions can overcome any limitation posed by the *EPOC* phenomenon. First, the combined effect of temperature and *EPOC* was investigated. It was found that with increase in temperature, the chain growth probability decreases. Thus, at higher temperature, products with low carbon numbers will be majorly formed. As shown in fig: 4.8, at temperature around 553.15 K, methane could be the only product. On the other hand temperature enhances the reaction rate. This can be helpful as alkali coverage on the catalyst reduces the magnitude of reaction rate. But, there is a trade off between reaction rate and chain growth probability. If one has to increase, the other will decrease. Increasing the operating temperature can be considered if products with low carbon number are desired.

Secondly, the influence of  $H_2 : CO$  ratio is studied on the reaction rate and chain growth probability. Assuming the *Yates and Satterfield* (eq: 3.9) expression is valid, it has been found that increasing the  $H_2 : CO$  ratio initially increases the reaction rate till it reaches a maximum and then it starts decreasing with further increase in the ratio. An intermediate ratio, where reaction rate is maximum can compensate to some extent the reduced magnitude of reaction rate due to *EPOC*. On the other hand chain growth probability is observed to be continuously decreasing with increasing  $H_2 : CO$  ratio. Reduction in the magnitude of the chain growth probability is due to the decrease in *CO* concentrations in the reactant feed. Thus, there are less number of carbon atoms available for chain growth. Reduction in chain growth probability can be improved with the application of more negative potential or higher alkali loading.

Next, effect of pressure has been studied in combination with *EPOC*. Increasing the pressure improves the reaction rate and at the same time increases the residence time of the reactor. This leads to an increase in the conversion of the reactants. But there is no influence of pressure on the chain growth probability. Increase in operating pressure will be helpful in improving the reaction rate which was reduced due to alkali loading.

## 5.2 Dynamic Electrochemical Promotion of Catalysis

The effect of periodic application of potential has been studied to investigate whether the periodicity affects the reactant conversion, selectivity of carbon chains and olefin-paraffin ratio. Influence of the frequency, symmetry or duty cycle and amplitude of the periodic wave has been studied.

Influence of frequency of the input potential signal on the coverage of the promoter ions on the catalyst surface have been studied. The application of high frequency can be limited by the slow diffusive transport of ions to the catalyst surface. At very high frequency, the promoter ions will not be able to capture the effect of frequency. But, with smaller thickness of the catalyst, higher frequency of periodicity can be applied. This is because the diffusive time scale gets reduced with decreasing catalyst film thickness.

Next the effect of frequency has been studied on *FT* reaction. It has been observed that with the increase in frequency, *CO* conversion and *CH<sub>4</sub>* selectivity increases first, on reaching a maximum, their corresponding magnitudes start descending. This could be due to the improvement in *H<sub>2</sub>* adsorption with initial increment in frequency. The decreasing values of *CO* conversion and *CH<sub>4</sub>* selectivity at higher frequency could be because of the mismatch between the time scale for the adsorption of *H<sub>2</sub>* and the frequency of the variation in the periodic potential. When compared to *CO* conversion and *CH<sub>4</sub>* selectivity, olefin-paraffin ratio for *C<sub>2</sub>* molecules showed exact opposite behaviour. A minima in the trend is observed where *H<sub>2</sub>* adsorption is possibly the highest. This is because with the increase in hydrogen adsorption, formation of paraffins increases.

Next, the influence of the duty cycle or symmetry has been studied. Here, the duty cycle was increased from 10% to 90%. Increasing the duty cycle means increasing the fraction of  $-0.4$  V within each cycle of the waveform. *CO* conversion decreases with the increase in the duty cycle. This is because, *CO* conversion depends on *H<sub>2</sub>* adsorption which decreases with the duty cycle. Similarly, the *CH<sub>4</sub>* selectivity decreases. This is because *CH<sub>4</sub>* is a hydrogenated product. Also, the production of paraffins decreases. As a result, selectivity of olefins increase which further increases the olefin paraffin ratio. Increasing the duty cycle increases the magnitude of chain growth probability. Thus, longer carbon chains can be expected to form. This happens because of enhancement in *CO* adsorption with increasing duty cycle. Also a comparison was made between *DEPOC* and *EPOC* by choosing a symmetrical periodic potential wave with a frequency of 0.001 Hz and its corresponding average potential. Higher *CO* conversion and *CH<sub>4</sub>* selectivity were observed in *DEPOC* case as *H<sub>2</sub>* adsorption increases. Consequently, the *C<sub>2</sub>H<sub>4</sub>* : *C<sub>2</sub>H<sub>6</sub>* ratio was higher for the *EPOC* case. Thus, it is difficult to say which case is better. Everything will depend on the requirement.

Finally, the effect of amplitude has been investigated. With the increase in the amplitude, hydrogen adsorption increases slightly. This happens because, each time the amplitude is increased, the maximum potential of the wave form increases. This value has a greater influence because the adsorption of *H<sub>2</sub>* has an exponential dependence on the applied potential. Increasing the amplitude, increases the *CO* conversion and *CH<sub>4</sub>* selectivity but reduces the olefin paraffin ratio and chain growth probability. The variations are not significantly large which is due to the assumption of a lower value of charge transfer coefficient of *H<sub>2</sub>*.

## 5.3 Reactor Design

Since, the basic structure of the reactor cells used in *EPOC* are identical to *SOFc* cells, these type of reactors are promising candidate for scaling up. Another possibility is the monolith type reactors. Even hybrid combinations of flat plate *SOFc* type cells arranged in a monolithic structure have been studied for the reduction of *NO<sub>x</sub>* using ethylene in presence of *O<sub>2</sub>* [100]. But the main challenge is the extremely low activity per unit mass of the catalyst compared to the catalyst designs used in conventional reactors. To overcome this research on

thin nanostructured catalyst films have been researched [100]. Another issue is the presence of many wired connections in the reactor. For this designs of the reactors can get complicated. Therefore, wireless design concepts like bipolar configuration [104] and the use of mixed ionic conducting membranes [105] for transfer of ions have been researched.

Comparison between the reactant conversion in *EPOC* and conventional case for *FT* has been shown in fig: 4.21. With such low activity in the case of *EPOC*, it will be difficult to think about scaling up of the process.

If the activity of the catalyst is improved then, another crucial issue will be heat management. Fischer Tropsch is a highly exothermic reaction, because of which it releases large amount of heat. This leads to rise in temperature along the length of the reactor which affects the selectivity of the reaction. This is because with increase in temperature, chain growth probability will decrease. Thus, non isothermal operation will lead to the formation of low carbon number products.

## 5.4 Future Outlook

There are very few literature on the effect of *EPOC* on *FT* reaction. Further studies on this topic is necessary. Understanding the mechanism of the reactions taking place on the promoted surface is important. Detailed theoretical analysis is required to elucidate these mechanisms. Moreover, the works on electrochemical promotion for *FT* are mostly based on alkali promotion. Investigating the effect of anionic promoters could be an interesting topic.

For the case of periodic application of the *EPOC* effect, more elaborate analysis is required. Most importantly, proper experiments are needed to understand the phenomenon. It is also crucial to thoroughly understand the limitations on the application of high frequency caused by the diffusive time scale. At the same time, micro-kinetic analysis needs to be done for understanding the changes taking place in the elementary reactions due to the periodic variations in the applied potential.

Another aspect is to perform a detailed study of reactor design for electrochemically promoted *FT* process and also in general for *EPOC*. Concepts from already proven technologies like batteries, electrolyzers and fuel cells can be adopted [106]. Also, challenges like lower activity per unit mass of the catalyst, complications in designing due to large number of wired connections have to be dealt with while considering reactor design.

Prefeasibility studies are necessary to understand the opportunities and limitations of this phenomenon at commercial scale. This should include system level studies, taking into account for all the operating processes.



# Bibliography

- [1] Q. Wang, ed., *Post-combustion Carbon Dioxide Capture Materials*, Inorganic Materials Series (The Royal Society of Chemistry, 2019) pp. P001–307.
- [2] R. Stanger, T. Wall, R. Spörl, M. Paneru, S. Grathwohl, M. Weidmann, G. Scheffknecht, D. McDonald, K. Myöhänen, J. Ritvanen, *et al.*, *Oxyfuel combustion for co<sub>2</sub> capture in power plants*, *International Journal of Greenhouse Gas Control* **40**, 55 (2015).
- [3] D. Jansen, M. Gazzani, G. Manzolini, E. van Dijk, and M. Carbo, *Pre-combustion co<sub>2</sub> capture*, *International Journal of Greenhouse Gas Control* **40**, 167 (2015).
- [4] R. Schlögl, C. Abanades, M. Aresta, A. Azapagic, E. A. Blekkan, T. Cantat, G. Centi, N. Duic, A. El Khamlichi, G. Hutchings, *et al.*, *Novel carbon capture and utilisation technologies: Research and climate aspects*, (2018).
- [5] H. Herzog, D. Golomb, *et al.*, *Carbon capture and storage from fossil fuel use*, *Encyclopedia of energy* **1**, 277 (2004).
- [6] S. Dang, H. Yang, P. Gao, H. Wang, X. Li, W. Wei, and Y. Sun, *A review of research progress on heterogeneous catalysts for methanol synthesis from carbon dioxide hydrogenation*, *Catalysis Today* **330**, 61 (2019).
- [7] S. Nitopi, E. Bertheussen, S. B. Scott, X. Liu, A. K. Engstfeld, S. Horch, B. Seger, I. E. Stephens, K. Chan, C. Hahn, *et al.*, *Progress and perspectives of electrochemical co<sub>2</sub> reduction on copper in aqueous electrolyte*, *Chemical reviews* **119**, 7610 (2019).
- [8] R. Küngas, *Electrochemical co<sub>2</sub> reduction for co production: Comparison of low-and high-temperature electrolysis technologies*, *Journal of The Electrochemical Society* **167**, 044508 (2020).
- [9] S. van Bavel, S. Verma, E. Negro, and M. Bracht, *Integrating co<sub>2</sub> electrolysis into the gas-to-liquids–power-to-liquids process*, *ACS Energy Letters* **5**, 2597 (2020).
- [10] H. Mahmoudi, M. Mahmoudi, O. Doustdar, H. Jahangiri, A. Tsolakis, S. Gu, and M. LechWyszynski, *A review of fischer tropsch synthesis process, mechanism, surface chemistry and catalyst formulation*, *Biofuels Engineering* **2**, 11 (2017).
- [11] Y. Zheng, J. Wang, B. Yu, W. Zhang, J. Chen, J. Qiao, and J. Zhang, *A review of high temperature co-electrolysis of h<sub>2</sub>o and co<sub>2</sub> to produce sustainable fuels using solid oxide electrolysis cells (soecs): advanced materials and technology*, *Chemical Society Reviews* **46**, 1427 (2017).
- [12] M. Matsuka, R. D. Braddock, T. Hanaoka, K. Shimura, T. Miyazawa, and S. Hirata, *Effect of process-condition-dependent chain growth probability and methane formation on modeling of the fischer–tropsch process*, *Energy & Fuels* **30**, 7971 (2016).
- [13] H. Jahangiri, J. Bennett, P. Mahjoubi, K. Wilson, and S. Gu, *A review of advanced catalyst development for fischer–tropsch synthesis of hydrocarbons from biomass derived syn-gas*, *Catalysis Science & Technology* **4**, 2210 (2014).
- [14] D. Pal, R. Chand, S. Upadhyay, and P. Mishra, *Performance of water gas shift reaction catalysts: A review*, *Renewable and Sustainable Energy Reviews* **93**, 549 (2018).

- [15] N. Cherkasov, A. Ibhaddon, and P. Fitzpatrick, *A review of the existing and alternative methods for greener nitrogen fixation*, *Chemical Engineering and Processing: Process Intensification* **90**, 24 (2015).
- [16] Y. Matsumura and T. Nakamori, *Steam reforming of methane over nickel catalysts at low reaction temperature*, *Applied Catalysis A: General* **258**, 107 (2004).
- [17] J. A. Cracknell, K. A. Vincent, and F. A. Armstrong, *Enzymes as working or inspirational electrocatalysts for fuel cells and electrolysis*, *Chemical Reviews* **108**, 2439 (2008).
- [18] O. T. Holton and J. W. Stevenson, *The role of platinum in proton exchange membrane fuel cells*, *Platinum Metals Review* **57**, 259 (2013).
- [19] G. Rothenberg, *Catalysis: concepts and green applications* (John Wiley & Sons, 2017).
- [20] A. Balandin, *Modern state of the multiplet theory of heterogeneous catalysis*, in *Advances in catalysis*, Vol. 19 (Elsevier, 1969) pp. 1–210.
- [21] C. G. Vayenas, S. Bebelis, C. Pliangos, S. Brosda, and D. Tsiplakides, *Electrochemical activation of catalysis: promotion, electrochemical promotion, and metal-support interactions* (Springer Science & Business Media, 2001).
- [22] C. Vayenas, S. Brosda, and C. Pliangos, *Rules and mathematical modeling of electrochemical and chemical promotion: 1. reaction classification and promotional rules*, *Journal of Catalysis* **203**, 329 (2001).
- [23] S. Brosda and C. Vayenas, *Rules and mathematical modeling of electrochemical and classical promotion: 2. modeling*, *Journal of Catalysis* **208**, 38 (2002).
- [24] J. Poppe, S. Völkening, A. Schaak, E. Schütz, J. Janek, and R. Imbihl, *Electrochemical promotion of catalytic CO oxidation on Pt/YSZ catalysts under low pressure conditions*, *Physical Chemistry Chemical Physics* **1**, 5241 (1999).
- [25] A. Toghan, L. M. Rösken, and R. Imbihl, *The electrochemical promotion of ethylene oxidation at a Pt/YSZ catalyst*, *ChemPhysChem* **11**, 1452 (2010).
- [26] A. Palermo, M. S. Tikhov, N. C. Filkin, R. M. Lambert, I. V. Yentekakis, and C. G. Vayenas, *Electrochemical promotion of NO reduction by CO and by propene*, in *Studies in Surface Science and Catalysis*, Vol. 101 (Elsevier, 1996) pp. 513–522.
- [27] S. Neophytides, D. Tsiplakides, P. Stonehart, M. Jaksic, and C. Vayenas, *Electrochemical enhancement of a catalytic reaction in aqueous solution*, *Nature* **370**, 45 (1994).
- [28] S. Neophytides, D. Tsiplakides, P. Stonehart, M. Jaksic, and C. Vayenas, *Non-faradaic electrochemical modification of the catalytic activity of Pt for H<sub>2</sub> oxidation in aqueous alkaline media*, *The Journal of Physical Chemistry* **100**, 14803 (1996).
- [29] F. Cai, D. Gao, H. Zhou, G. Wang, T. He, H. Gong, S. Miao, F. Yang, J. Wang, and X. Bao, *Electrochemical promotion of catalysis over Pd nanoparticles for CO<sub>2</sub> reduction*, *Chemical Science* **8**, 2569 (2017).
- [30] G. Foti, V. Stanković, I. Bolzonella, and C. Comninellis, *Transient behavior of electrochemical promotion of gas-phase catalytic reactions*, *Journal of Electroanalytical Chemistry* **532**, 191 (2002).
- [31] R. R. Hudgins and P. L. Silveston, *Chapter 2 - hydrogenation processes*, in *Periodic Operation of Chemical Reactors*, edited by P. Silveston and R. Hudgins (Butterworth-Heinemann, Oxford, 2013) pp. 23 – 47.
- [32] R. R. Hudgins, P. L. Silveston, A. Renken, and Y. S. Matros, *Chapter 1 - introduction*, in *Periodic Operation of Chemical Reactors*, edited by P. Silveston and R. Hudgins (Butterworth-Heinemann, Oxford, 2013) pp. 1 – 22.
- [33] E. Pérez-Gallent, C. Sánchez-Martínez, L. F. Geers, S. Turk, R. Latsuzbaia, and E. L. Goetheer, *Overcoming mass transport limitations in electrochemical reactors with a pulsating flow electrolyzer*, *Industrial & Engineering Chemistry Research* **59**, 5648 (2020).

- [34] M. Chandrasekar and M. Pushpavanam, *Pulse and pulse reverse plating—conceptual, advantages and applications*, *Electrochimica Acta* **53**, 3313 (2008).
- [35] P. S. Fedkiw and W. D. Scott Jr, *Selectivity changes in electrochemical reaction sequences by modulated potential control*, *Journal of the Electrochemical Society* **131**, 1304 (1984).
- [36] P. Fedkiw and J. Chao, *Selectivity modification in electroorganic reactions by periodic current control: Electroreduction of nitrobenzene*, *AIChE journal* **31**, 1578 (1985).
- [37] D.-T. Chin and C. Cheng, *Oxidation of phenol with ac electrolysis*, *Journal of the Electrochemical Society* **132**, 2605 (1985).
- [38] M. A. Ardagh, O. A. Abdelrahman, and P. J. Dauenhauer, *Principles of dynamic heterogeneous catalysis: surface resonance and turnover frequency response*, *ACS Catalysis* **9**, 6929 (2019).
- [39] M. A. Ardagh, M. Shetty, A. Kuznetsov, Q. Zhang, P. Christopher, D. G. Vlachos, O. A. Abdelrahman, and P. J. Dauenhauer, *Catalytic resonance theory: parallel reaction pathway control*, *Chemical Science* **11**, 3501 (2020).
- [40] F. King, E. Shutt, and A. Thomson, *Ruthenium catalyst systems for the production of hydrocarbons from coal*, *Platinum Metals Rev* **29**, 146 (1985).
- [41] I. Kalaitzidou, A. Katsaounis, T. Norby, and C. Vayenas, *Electrochemical promotion of the hydrogenation of co<sub>2</sub> on ru deposited on a bzy proton conductor*, *Journal of Catalysis* **331**, 98 (2015).
- [42] D. Zagoraios, A. Athanasiadi, I. Kalaitzidou, S. Ntais, A. Katsaounis, A. Caravaca, P. Vernoux, and C. Vayenas, *Electrochemical promotion of methane oxidation over nanodispersed pd/co<sub>3o4</sub> catalysts*, *Catalysis Today* (2019).
- [43] S. Bebelis, H. Karasali, and C. Vayenas, *Electrochemical promotion of co<sub>2</sub> hydrogenation on rh/ysz electrodes*, *Journal of Applied Electrochemistry* **38**, 1127 (2008).
- [44] C. Vayenas and D. Tsipalakes, *On the work function of the gas-exposed electrode surfaces in solid state electrolyte cells*, *Surface science* **467**, 23 (2000).
- [45] I. S. Metcalfe, *Electrochemical promotion of catalysis: I: Thermodynamic considerations*, *Journal of Catalysis* **199**, 247 (2001).
- [46] E. Leiva, *On the work function changes and other properties of the gas-exposed electrode surface in the nemca effect*, *Topics in Catalysis* **44**, 347 (2007).
- [47] G. Pacchioni, F. Illas, S. Neophytides, and C. G. Vayenas, *Quantum-chemical study of electrochemical promotion in catalysis*, *The Journal of Physical Chemistry* **100**, 16653 (1996).
- [48] I. S. Metcalfe, *Electrochemical promotion of catalysis: the use of transition state theory for the prediction of reaction rate modification*, *Solid state ionics* **152**, 669 (2002).
- [49] I. M. Campbell, *Catalysis at surfaces* (Springer Science & Business Media, 1988).
- [50] F. J. Williams and R. M. Lambert, *A study of sodium promotion in fischer–tropsch synthesis: electrochemical control of a ruthenium model catalyst*, *Catalysis letters* **70**, 9 (2000).
- [51] A. J. Urquhart, F. J. Williams, and R. M. Lambert, *Electrochemical promotion by potassium of rh-catalysed fischer–tropsch synthesis at high pressure*, *Catalysis letters* **103**, 137 (2005).
- [52] A. Nakos, S. Souentie, and A. Katsaounis, *Electrochemical promotion of methane oxidation on rh/ysz*, *Applied Catalysis B: Environmental* **101**, 31 (2010).
- [53] S. Bebelis and C. Vayenas, *Non-faradaic electrochemical modification of catalytic activity: 1. the case of ethylene oxidation on pt*, *Journal of Catalysis* **118**, 125 (1989).
- [54] A. Kaloyannis and C. G. Vayenas, *Non-faradaic electrochemical modification of catalytic activity*, *Journal of Catalysis* **171**, 148 (1997).

- [55] P. Tsiakaras and C. Vayenas, *Non-faradaic electrochemical modification of catalytic activity: Vii. the case of methane oxidation on platinum*, *Journal of Catalysis* **140**, 53 (1993).
- [56] C. Pliangos, I. Yentekakis, X. Verykios, and C. Vayenas, *Non-faradaic electrochemical modification of catalytic activity*, *J. Catal* **154**, 124-136 (1995).
- [57] J. K. Hong, I.-H. Oh, S.-A. Hong, and W. Y. Lee, *Electrochemical oxidation of methanol over a silver electrode deposited on yttria-stabilized zirconia electrolyte*, *Journal of Catalysis* **163**, 95 (1996).
- [58] I. Yentekakis, Y. Jiang, S. Neophytides, S. Bebelis, and C. Vayenas, *Catalysis, electrocatalysis and electrochemical promotion of the steam reforming of methane over ni film and ni-ysz cermet anodes*, *Ionics* **1**, 491 (1995).
- [59] M. Marwood and C. Vayenas, *Electrochemical promotion of the catalytic reduction of no by co on palladium*, *Journal of Catalysis* **170**, 275 (1997).
- [60] C. Vayenas, S. Bebelis, and M. Despotopoulou, *Non-faradaic electrochemical modification of catalytic activity 4. the use of  $\beta$ - $\text{Al}_2\text{O}_3$  as the solid electrolyte*, *Journal of Catalysis* **128**, 415 (1991).
- [61] O. Marina, I. Yentekakis, C. Vayenas, A. Palermo, and R. Lambert, *In situ controlled promotion of catalyst surfaces via nemca: The effect of na on the pt-catalyzed no reduction by h<sub>2</sub>*, *Journal of Catalysis* **166**, 218 (1997).
- [62] C. Karavasilis, S. Bebelis, and C. Vayenas, *In situ controlled promotion of catalyst surfaces via nemca: The effect of na on the ag-catalyzed ethylene epoxidation in the presence of chlorine moderators*, *Journal of Catalysis* **160**, 205 (1996).
- [63] W. Becker, R. Braun, M. Penev, and M. Melaina, *Production of fischer-tropsch liquid fuels from high temperature solid oxide co-electrolysis units*, *Energy* **47**, 99 (2012).
- [64] R. H. Williams, E. D. Larson, G. Liu, and T. G. Kreutz, *Fischer-tropsch fuels from coal and biomass: Strategic advantages of once-through ("polygeneration") configurations*, *Energy Procedia* **1**, 4379 (2009).
- [65] A. Kotsiras, I. Kalaitzidou, D. Grigoriou, A. Symillidis, M. Makri, A. Katsaounis, and C. Vayenas, *Electrochemical promotion of nanodispersed ru-co catalysts for the hydrogenation of co<sub>2</sub>*, *Applied Catalysis B: Environmental* **232**, 60 (2018).
- [66] D. Grigoriou, D. Zagoraios, A. Katsaounis, and C. Vayenas, *The role of the promoting ionic species in electrochemical promotion and in metal-support interactions*, *Catalysis Today* (2019).
- [67] F. J. Williams, A. Palermo, S. Tracey, M. S. Tikhov, and R. M. Lambert, *Electrochemical promotion by potassium of the selective hydrogenation of acetylene on platinum: reaction studies and xp spectroscopy*, *The Journal of Physical Chemistry B* **106**, 5668 (2002).
- [68] M. Makri, A. Symillidis, D. Grigoriou, A. Katsaounis, and C. Vayenas, *Electrochemical promotion of co<sub>2</sub> reduction on a dispersed ru/ysz catalyst supported on ysz solid electrolyte*, *Materials Today: Proceedings* **5**, 27617 (2018).
- [69] F. Fischer and H. Tropsch, *About the production of synthetic oil mixtures (synthol) by construction from carbon oxide and hydrogen*, *Brennst. Chem* **4**, 276 (1923).
- [70] A. de Klerk, *Fischer-tropsch process*, *Kirk-Othmer Encyclopedia of Chemical Technology*, 1 (2000).
- [71] C. Maretto and R. Krishna, *Modelling of a bubble column slurry reactor for fischer-tropsch synthesis*, *Catalysis today* **52**, 279 (1999).
- [72] S. Czernik and A. Bridgwater, *Overview of applications of biomass fast pyrolysis oil*, *Energy & fuels* **18**, 590 (2004).
- [73] Y. Zhao, *On the investigation of alcohol synthesis via the Fischer Tropsch reaction* (Cardiff University (United Kingdom), 2007).

- [74] R. Espinoza, A. Steynberg, B. Jager, and A. Vosloo, *Low temperature fischer–tropsch synthesis from a sasol perspective*, Applied Catalysis A: General **186**, 13 (1999).
- [75] G. P. van der Laan, *Kinetics, selectivity and scale up of the Fischer-Tropsch synthesis* (Groningen, 1999).
- [76] M. Post, A. Van't Hoog, J. Minderhoud, and S. Sie, *Diffusion limitations in fischer-tropsch catalysts*, AIChE Journal **35**, 1107 (1989).
- [77] I. C. Yates and C. N. Satterfield, *Intrinsic kinetics of the fischer-tropsch synthesis on a cobalt catalyst*, Energy & fuels **5**, 168 (1991).
- [78] E. Iglesia, S. C. Reyes, and S. L. Soled, *Reaction-transport selectivity models and*, Computer-aided design of catalysts **51**, 199 (1993).
- [79] F. Campanario and F. G. Ortiz, *Fischer-tropsch biofuels production from syngas obtained by supercritical water reforming of the bio-oil aqueous phase*, Energy Conversion and Management **150**, 599 (2017).
- [80] H.-S. Song, D. Ramkrishna, S. Trinh, and H. Wright, *Operating strategies for fischer-tropsch reactors: A model-directed study*, Korean Journal of Chemical Engineering **21**, 308 (2004).
- [81] E. Iglesia, S. C. Reyes, and R. J. Madon, *Transport-enhanced  $\alpha$ -olefin readsorption pathways in ru-catalyzed hydrocarbon synthesis*, Journal of Catalysis **129**, 238 (1991).
- [82] T. Okuhara, H. Tamura, and M. Misono, *Effect of potassium and phosphorus on the hydrogenation of co over alumina-supported ruthenium catalyst*, Journal of Catalysis **95**, 41 (1985).
- [83] S. Hedrick, S. Chuang, A. Pant, and A. Dastidar, *Activity and selectivity of group viii, alkali-promoted mn-ni, and mo-based catalysts for c2+ oxygenate synthesis from the co hydrogenation and co/h2/c2h4 reactions*, Catalysis today **55**, 247 (2000).
- [84] A. J. Urquhart, J. M. Keel, F. J. Williams, and R. M. Lambert, *Electrochemical promotion by potassium of rhodium-catalyzed fischer-tropsch synthesis: Xp spectroscopy and reaction studies*, The Journal of Physical Chemistry B **107**, 10591 (2003).
- [85] A. Nikolopoulos, S. Gangwal, and J. Spivey, *Effect of periodic pulsed operation on product selectivity in*, Natural Gas Conversion VI, 351 (2001).
- [86] A. A. Adesina, R. R. Hudgins, and P. L. Silveston, *Influence of concentration waves on the fischer–tropsch reaction*, Journal of Chemical Technology & Biotechnology **50**, 535 (1991).
- [87] F. Dautzenberg, J. Helle, R. Van Santen, and H. Verbeek, *Pulse-technique analysis of the kinetics of the fischer-tropsch reaction*, Journal of Catalysis **50**, 8 (1977).
- [88] P. Silveston, R. Hudgins, A. Adesina, G. Ross, and J. Feimer, *Activity and selectivity control through periodic composition forcing over fischer-tropsch catalysts*, Chemical engineering science **41**, 923 (1986).
- [89] A. Adesina, R. Hudgins, and P. Silveston, *Feed composition modulation of hydrocarbon synthesis over a cobalt oxide catalyst*, The Canadian Journal of Chemical Engineering **64**, 447 (1986).
- [90] J. Feimer, P. Silveston, and R. Hudgins, *Influence of forced cycling on the fischer-tropsch synthesis. part ii. response to feed concentration square-waves*, The Canadian Journal of Chemical Engineering **63**, 86 (1985).
- [91] J. Hölzl and F. K. Schulte, *Work function of metals*, in *Solid surface physics* (Springer, 1979) pp. 1–150.
- [92] R. M. De Deugd, *Fischer-tropsch synthesis revisited; efficiency and selectivity benefits from imposing temporal and/or spatial structure in the reactor*, (2004).
- [93] D. Vervloet, F. Kapteijn, J. Nijenhuis, and J. R. van Ommen, *Fischer–tropsch reaction–diffusion in a cobalt catalyst particle: aspects of activity and selectivity for a variable chain growth probability*, Catalysis Science & Technology **2**, 1221 (2012).
- [94] E. Kuipers, I. Vinkenburg, and H. Oosterbeek, *Chain length dependence of  $\alpha$ -olefin readsorption in fischer-tropsch synthesis*, Journal of Catalysis **152**, 137 (1995).

- [95] B. Todic, T. Bhatelia, G. F. Froment, W. Ma, G. Jacobs, B. H. Davis, and D. B. Bukur, *Kinetic model of fischer–tropsch synthesis in a slurry reactor on co–re/al<sub>2</sub>o<sub>3</sub> catalyst*, *Industrial & Engineering Chemistry Research* **52**, 669 (2013).
- [96] J. Udagawa, P. Aguiar, and N. Brandon, *Hydrogen production through steam electrolysis: Model-based steady state performance of a cathode-supported intermediate temperature solid oxide electrolysis cell*, *Journal of Power Sources* **166**, 127 (2007).
- [97] M. Andersson, *Solid Oxide Fuel Cell Modeling at the Cell Scale-Focusing on Species, Heat, Charge and Momentum Transport as well as the Reaction Kinetics and Effects* (Lund University, 2011).
- [98] F. J. Williams, A. Palermo, M. S. Tikhov, and R. M. Lambert, *The origin of electrochemical promotion in heterogeneous catalysis: Photoelectron spectroscopy of solid state electrochemical cells*, *The Journal of Physical Chemistry B* **104**, 615 (2000).
- [99] C. Vayenas and G. Pitselis, *Mathematical modeling of electrochemical promotion and of metal- support interactions*, *Industrial & engineering chemistry research* **40**, 4209 (2001).
- [100] S. Balomenou, D. Tsiplakides, A. Katsaounis, S. Thiemann-Handler, B. Cramer, G. Foti, C. Comninellis, and C. Vayenas, *Novel monolithic electrochemically promoted catalytic reactor for environmentally important reactions*, *Applied Catalysis B: Environmental* **52**, 181 (2004).
- [101] T. Tagawa, K. Kuroyanagi, S. Goto, S. Assabumrungrat, and P. Praserttham, *Selective oxidation of methane in an sofc-type reactor: effect of applied potential*, *Chemical Engineering Journal* **93**, 3 (2003).
- [102] J. O'Brien, C. Stoots, V. Sharma, B. Yildiz, and A. Virkar, *Degradation Issues in Solid Oxide Cells During High Temperature Electrolysis*, Tech. Rep. (Idaho National Laboratory (INL), 2010).
- [103] D. Tsiplakides and S. Balomenou, *Electrochemical promoted catalysis: towards practical utilization*, *Chemical Industry and Chemical Engineering Quarterly* **14**, 97 (2008).
- [104] S. Balomenou, G. Pitselis, D. Polydoros, A. Giannikos, A. Vradis, A. Frenzel, C. Pliangos, H. Pütter, and C. Vayenas, *Electrochemical promotion of pd, fe and distributed pt catalyst-electrodes*, *Solid State Ionics* **136**, 857 (2000).
- [105] D. Poulidi, A. Thursfield, and I. Metcalfe, *Electrochemical promotion of catalysis controlled by chemical potential difference across a mixed ionic-electronic conducting ceramic membrane—an example of wireless nemca*, *Topics in Catalysis* **44**, 435 (2007).
- [106] N. A. Anastasijevic, *Nemca—from discovery to technology*, *Catalysis Today* **146**, 308 (2009).